WIND TUNNEL STUDIES OF THE PRESSURE DISTRIBUTION AND THE FLOW FIELD IN THE WAKE OF THE LOCKHEED C-141A STARLIFTER JET TRANSPORT AIRCRAFT

T. F. GOODRICK

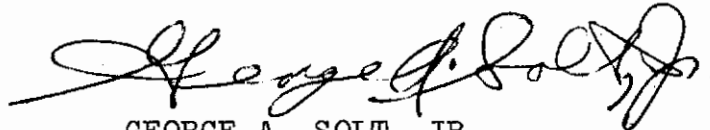*** Export controls have been removed ***

FOREWORD

This report was prepared by the Department of Aeronautics and Engineering Mechanics of the University of Minnesota in compliance with U. S. Air Force Contract No. F33615-67-C-1010, "Theoretical Deployable Aerodynamic Decelerator Investigations," Task 606503, "Parachute Aerodynamics and Structures," Project 6065, "Performance and Design of Deployable Aerodynamic Decelerators." The work for this report was performed between August 1, 1966 and July 31, 1967.

The work accomplished under this contract was sponsored jointly by U. S. Army Natick Laboratory, Department of the Army; Bureau of Aeronautics and Bureau of Ordnance, Department of the Navy; and Air Force Systems Command, Department of the Air Force, and was directed by a Tri-Service Steering Committee concerned with Aerodynamic Retardation. The work was administered under the direction of the Recovery and Crew Station Branch, Air Force Flight Dynamics Laboratory, Research and Technology Division. Mr. James DeWeese was the project engineer.

The study was conducted under the direction of Professor H. G. Heinrich and in cooperation with Messrs. E. L. Haak, R. J. Niccum and R. A. Noreen. Several students of Aerospace Engineering of the University of Minnesota participated in the performance of the tests and data reduction. The author wishes to express his gratitude to all who rendered their services to the accomplishment of this work.

The manuscript was released by the author in August 1967 for publication.

This technical report has been reviewed and is approved.

GEORGE A. SOLT, JR.
Chief, Recovery and Crew Station Branch
AF Flight Dynamics Laboratory

ii

ABSTRACT

Wind tunnel studies of a 1:56 scale non-powered model of the Lockheed C-141A Starlifter jet transport indicate the following characteristics of the flow field which affect the deployment of paratroops and cargo from the side doors and from the rear cargo ramp: a 15° to 20° down-wash occurs across the side doors when the petal doors are closed, the flow beneath the side doors is inclined toward the centerline approximately 30°; and a 20° to 40° upwash occurs between and behind the petal doors when the doors are open 65°. An analytic approximation of the effect of engine exhaust on the wake shows that the performance of a single parachute may not be significantly affected, but that of clustered extraction parachutes would be influenced by the engine slipstream.

The distribution of this Abstract is unlimited.

TABLE OF CONTENTS

iv

ILLUSTRATIONS

vi

TABLES

SYMBOLS

A	cross-sectional area
$\mathcal{R}$	aspect ratio
C_{D_f}	friction drag coefficient
C_L	lift coefficient
C_p	pressure coefficient
D	drag
e	Oswald's efficiency factor ($\doteq 0.85$)
F	net thrust (fuel flow neglected)
H	height of aircraft
K	jet spreading parameter ($\doteq 0.0124$)
L	length of aircraft
$\dot{m}$	mass flow
p	static pressure
p_t	total pressure
q	dynamic pressure
$\bar{R}$	gas constant ($\doteq 1716 \ \text{ft}^2/\text{sec}^2 \ ^\circ R$)
R	radius of jet boundary at x
r	radial distance from jet axis
$\bar{S}$	wing span of aircraft
S	wing area
T	temperature
T_c	thrust coefficient
U	increment of jet velocity over stream velocity at point x on jet axis ($V_j - V$)
u	increment of jet velocity over stream velocity at point (x,r)

V	stream velocity
V_j	jet velocity
X	longitudinal coordinate
x	axial distance from point at which jet would have zero cross section
Y	lateral coordinate
Z	vertical coordinate
γ	ratio of specific heats ($\doteq$ 1.4)
η	$= R\sqrt{\dfrac{\pi\, I_1^2/I_2}{ST_c}}$
θ	tangential coordinate
ρ	density
τ	time
ϕ	volume of reservoir

Subscripts:

e	exit conditions
m	model
o	conditions when $\tau = 0$
p	prototype
t	total conditions
1	primary reservoir condition
2	secondary reservoir condition
*	throat conditions
∞	freestream conditions

I.   SURFACE PRESSURE AND FLOW FIELD

A.   Introduction

The C-141A Starlifter is a four-engine jet transport airplane capable of carrying and releasing airborne troops and airborne cargo. Its cruising speed is approximately 500 mph with an airdrop speed between 135 and 230 mph.

In initial drop tests certain undesirable parachute deployment and inflation characteristics have been observed, and it is the purpose of these wind tunnel experiments to study the surface flow field near the stern of the Lockheed C-141A aircraft and to determine which characteristics of the flow field may adversely affect the deployment of personnel and cargo parachutes from the side doors and from the rear cargo ramp. With this objective in mind, measurements of the static pressure distribution on the surfaces of the fuselage and cargo doors were made and correlated with photographs of tufts representing streamlines in the same regions. The experiments were made on a 1:56 scale model with petal doors both closed and open 65°. The wind tunnel speed was varied between 150 and 250 fps.

B.   Model Design

The 1:56 scale model using the drawings of Ref 1, is made of mahogany and aluminum (Figs 1 and 2). The engine pods are hollow to simulate feathered engines. Two sections- one with cargo doors closed and one with cargo doors open 65°- fit interchangeably into a cutout in the stern. The model was mounted in the tunnel without obstructing the flow beneath or adjacent to either side of the model (Fig 2). The coordinate system used for data presentation is shown in Fig 3.

For measurement of the static pressure distribution on the surface, twenty-four 0.017 in. I.D. pressure taps were installed in the surfaces of the fuselage and the petal doors on both the open and closed-door stern sections. The taps were arranged in a helical pattern on the left side and bottom of the stern, with sufficient taps on the right side to insure that the flow was symmetrical. Taps were also installed on the inner surfaces of the open petal doors.

For flow visualization, tufts of white floss were taped to the surfaces in a pattern corresponding to the pressure taps.

C.   Test Procedure

The static pressure taps were connected to manometer boards which were photographed to insure simultaneity. The

1

tufted model was photographed simultaneously from the side and from below the test section to allow three-dimensional analysis of the streamlines. Tests were conducted at wind tunnel speeds of 150, 175, 190, 210, 220, 230, and 245 fps. Pressure data was reduced to pressure coefficient form where

$$C_p = \frac{p - p_\infty}{q_\infty}$$

D.   Results

1.   Closed-door Configuration

The surface pressure studies (Figs 4, 5, and 6, Table I) and the corresponding tuft studies (Fig 7) show a 15° to 20° downwash across the side doors with the flow under these doors inclined toward the centerline approximately 30° (The side doors are located at the vertical line showing the joint of the removable section, Fig 7.).

2.   Open-door Configuration

The surface pressure studies (Figs 8 and 9) and the tuft studies (Figs 10 and 11) show a 20° to 40° upwash between and behind the petal doors. The surface pressure studies (Table I, Fig 8) show the pressure differential which causes the suction near the ramp. The effects of the suction can be seen in the tuft studies (Fig 10). The pressure coefficient above the ramp in a stagnation region is -0.39 while the coefficients on the adjacent external surfaces range from -0.06 to +0.12.

Neither the tuft alignment nor the pressure coefficients vary significantly over the velocity range studied. The random variation of the pressure coefficients is less than ±2.5%.

E.   Conclusions

The characteristics of the flow field potentially capable of interfering with paratroop and cargo egress are the downwash, occurring across the side doors when the petal doors are closed, and the upwash, occurring between and below the open petal doors. In addition, the streamline pattern and pressure differential on the open-door configuration indicate that simultaneous drops from both side doors and ramp are not advisable. The results of these studies are in agreement with prototype experiments (Ref 2).

2

II.   WAKE FLOW FIELD WITHOUT ENGINE POWER

A.   Introduction

The second phase of the C-141A wind tunnel studies was the determination of the dynamic pressure distribution in the wake which affects cargo extraction from the ramp. Measurements were made of static and total pressures in a plane normal to the flow at four stations behind the aircraft in the region where extraction parachutes operate. In addition, a wire grid with tufts attached was photographed in the vertical plane at the rear tip of the horizontal stabilizer to determine the local variations in flow direction.

B.   Model Configuration

The model was the same as described in the preceding section; however, the petal doors were open 65° in all tests.

C.   Test Apparatus

A wake survey rake (Fig 12) effectively covering a twelve-inch span with both static and total pressure probes was connected to multimanometer boards.

D.   Test Procedure

The wake survey rake was placed horizontally across the tunnel at five vertical positions at each of four stations behind the model (Fig 13). The height of the region studied at each station represents 14 ft above and below the air-craft centerline, while the width of the region is 56 ft. This corresponds to the region through which the canopy of a 22-ft extraction parachute would pass. All tests were made at a freestream velocity of 200 fps since the results of Section I showed no variation with velocity.

E.   Results

A comparison of the dynamic pressure profiles at the four stations (Figs 14 to 18) and the photograph of the tufted grid (Fig 19) indicate that the most notable pressure defect occurs directly behind the petal doors. A region of low pressure, $q/q_\infty = 0.6$, and a 40° upwash exist directly behind the tail cone. Tabulated values of the pressure survey results are given in Tables II to V.

3

F.   Conclusions

      The pressure distribution shows that the flow field forms a low-velocity symmetrically-arranged region centrally behind the ramp. This will result in a reduced parachute extraction force. The existing upwash may cause the parachute to ride somewhat above the centerline. This explains observations made with the prototype aircraft.

III. WAKE FLOW FIELD WITH ENGINE POWER

A.   Introduction

The third phase of the C-141A studies concerned an analytical investigation of the effects of powered engines on the wake flow field and of the feasibility of simulating power on the 1:56 scale model. For steady, low-altitude flight at 200 fps, an approximation of the dynamic pressure distribution can be made based on the theoretical and experimental studies shown in Ref 3. The results of this analysis are readily compatible with the data of the non-powered wake survey presented in Section II above.

The analytical method of Ref 3 is used to determine: (1) the spreading of the jet; (2) the velocity variation along the jet axis; and (3) the radial velocity distribution. The parameters used in Ref 3 are dimensionless and can be applied for geometric and thrust scaling for the 1:56 scale model of the C-141A. The results of the analysis (Ref 3) may be presented in the form of dynamic pressure ratios $q(x,r)/q_\infty$. Experimental data in Section II shows virtual freestream conditions in the region of the airplane that is affected by engine power. Therefore, the analytical data of the power effects (Ref 3) may be superimposed upon the experimental data of the non-powered wake (Section II above). The analytical approximation assumes no thermal effects, as these are considered negligible under the specific flight conditions.

B.   Analytic Approximation

The spreading of the jet beyond eight diameters downstream of the nozzle is governed by the relation (Fig 20)

$$R^3 = K \cdot x \ . \tag{1}$$

By using equations obtained in Ref 3, the constant, K, in Eqn 1 was determined to be 0.0124 for the 1:56 scale model of the C-141A at $V_\infty \doteq 200$ fps.

The velocity variation along the jet axis is governed by the relation

$$\frac{U}{V} = \frac{I_1}{2I_2} \left(\sqrt{1 + \frac{1}{\eta^2}} - 1 \right) \tag{2}$$

where $I_1 = \displaystyle\int_0^1 \frac{u}{U} \frac{r}{R} \, d\left(\frac{r}{R}\right) .$

5

and
$$I_2 = \int_0^1 \left(\frac{u}{U}\right)^2 \frac{r}{R} \, d\left(\frac{r}{R}\right) .$$

The integrals I_1 and I_2 are determined by experiment (Ref 3) to be

$$I_1 = 0.0991$$

and
$$I_2 = 0.04895.$$

The radial velocity distribution within the jet may be determined from an experimental plot of u/U as a function of r/R for a turbojet engine (Fig 2 of Ref 3).

Since the results of Eqn 2 and the radial velocity distribution obtained graphically are given in the forms U/V and u/U, respectively, the results must be modified to the form of dynamic pressure ratios where

$$\frac{q(x,r)}{q_\infty} = \left(\frac{u}{U} \frac{U}{V} + 1\right)^2 \tag{3}$$

and
$$\frac{q(x,0)}{q_\infty} = \left(\frac{U}{V} + 1\right)^2 . \tag{4}$$

Hence, results applicable to the 1:56 scale model of the C-141A are obtained using the relations

$$R^3 = 0.0124x , \tag{1a}$$

$$\eta = \frac{R}{\sqrt{ST_c}} \sqrt{\frac{\pi I_1^2}{I_2}} = 2.98R \tag{5}$$

and
$$\frac{U}{V} = 1.01 \left(\sqrt{1 + \frac{1}{\eta^2}} - 1\right) . \tag{2a}$$

The scaled values of S and T_c are:

$$S = 1.03 \text{ ft}^2$$

$$T_c = 0.0690 \quad \text{(based on thrust per engine)}.$$

The results of this procedure, superimposed on the experimental results of the non-powered studies (Figs 21 to 24) show that the region affected by the jet blast overlaps the region through which a single parachute would pass. The jet blast from the engines, then, may have an effect on a single extraction parachute.

C.   Experimental Apparatus Design

The project specifications also requested the study of an experimental approach which would provide wind tunnel model conditions satisfactory for the investigation of the jet engine blast effects. The results of these effects are described in the following.

To satisfy similarity requirements, the cold air jet simulating a powered engine (Fig 25) must produce a thrust coefficient equal to that of the prototype while tested at a freestream velocity equal to the flight speed of the aircraft. If power is simulated by adding momentum from an external source, the thrust coefficient must be diminished by

$$\frac{V \dot{m}_{added}}{\frac{1}{2}\rho V^2 S}$$

to correct for this addition. The correction is neglected in the following analysis since the correction is less than 0.4%.

The required thrust of the prototype C-141A in steady, low altitude flight at 200 fps amounts to

$$F = D = (C_{D_f} + \frac{C_L^2}{\pi \mathcal{R} e}) \ (\frac{V^2}{391}) \ (S) \tag{6}$$

which is F = 10,600 lb/engine. With

$$T_c = \frac{F}{\frac{1}{2}\rho V^2 S} \ ,$$

$$T_{c_m} = T_{c_p} \ ,$$

and $S_m = (\frac{1}{56})^2 S_p \ ,$

the model thrust amounts to:

7

$$F_m = \frac{F_p}{3136} = \frac{\dot{m}_{e_p}(V_j - V)}{3136} \qquad (7)$$

Since the prototype engine has $\dot{m}_{e_p} = 15.5$ slugs/sec/engine with $V_{j_p} = 881$ fps, the model engine must provide, for the best similarity conditions

$$V_{j_m} = 881 \text{ fps}$$

and

$$\dot{m}_{e_m} = \dot{m}_{e_p}\left(\frac{1}{56}\right)^2 = 0.00494 \text{ slugs/sec/engine.}$$

Flow through a duct from a pressurized reservoir, however, has an inherent limitation governing the relationship between mass flow and exhaust velocity for any given exit area. To obtain a specific exit velocity each of the ratios, p_e/p_{t_2} and A_e/A_* must have a certain value. Since p_e is atmospheric pressure, and A_e is dimensionally scaled, the values of p_{t_2} and A_* are determined. However, the values of p_{t_2} and A_* determine the mass flow according to the relation

$$\dot{m}_e = \sqrt{\frac{\gamma}{R}\left(\frac{2}{\gamma+1}\right)^{\frac{\gamma+1}{\gamma-1}}} \; \frac{p_{t_2} A_*}{\sqrt{T_t}} \qquad (8)$$

or

$$\dot{m}_e = 0.000718 \, p_{t_2} A_*$$

for standard conditions and isentropic flow. Hence, it may not be possible to satisfy the similarity conditions of equal exhaust velocities, and scaled mass flow and area. However, Eqn 7 may be rearranged to give

$$V_j = \frac{F_m}{\dot{m}_{e_m}} + V_\infty \qquad (7a)$$

and Eqn 8 may be rearranged to give

$$\dot{m}_e = \frac{0.000718 \, A_e p_e}{\left(\frac{A_e}{A_*}\right)_{V_j}\left(\frac{p_e}{p_{t_2}}\right)_{V_j}} \qquad (8a)$$

where A_e/A_* and p_e/p_{t_2} are determined for any V_j from subsonic flow tables. Equations 7a and 8a may be solved simultaneously to determine values of V_j and $\dot{m}_e$ which satisfy both the similarity conditions and the flow requirements. For the present

8

case this method gives

$$V_j = 1,095 \text{ fps},$$

and $\quad \dot{m}_e = 0.00377 \text{ slugs/sec/engine}.$

To achieve these conditions with the system of Fig 25, the reservoir pressures must be

$$p_{t_2} = 27.0 \text{ psia },$$

$$p_{t_1} = 127.0 \text{ psia at } \mathcal{T} = 0 .$$

Considering starting pressure ratios and estimated pressure losses of about 58%, the amount of allowable testing time, governed by the loss of mass from the primary reservoir, is

$$\mathcal{T} = \frac{\phi_1}{\dot{m}_e \overline{R} T_t} \left(p_{t_{1_0}} - \frac{p_{t_2}}{0.42}\right) = 92 \text{ sec } . \tag{9}$$

The most practical test configuration for the power simulation apparatus (Fig 26) would be to have the secondary reservoir shaped in airfoil cross section and mounted upstream of the test section at a station of low velocity. A supply tube would extend to each nacelle. The primary reservoir, supply line, and pressure regulator would be outside the wind tunnel. If the diameter of the engine supply tubes were corrected for boundary layer buildup, little flow disturbance would be created. An alternate design, namely, to channel the exhaust air through the wings and pylons, would incur prohibitive pressure losses and is not considered to be advisable.

D. Conclusions

The analytic approximation yields results which may warrant its use for single parachutes in the wake, since the increase in slipstream dynamic pressure is gradual near its outer boundaries (Figs 21-24). This opinion is supported by full-size tow tests which showed no effects of jet engine exhausts upon the performance characteristics of the extraction parachute. In these tests, a 32-ft fist ribbon parachute was towed with an 80 ft line attached at fuselage Station 1260. This would place the plane of the canopy at about Station 2470 in the wake. According to the comments of the data sheet

9

(p. A-3 of Ref 2), there was "no effect on chute stability."
However, when clusters of parachutes are towed it seems quite
likely that the power effects may become significant. No
attempt has been made in this report to evaluate the total
effect of fuselage disturbances and slipstream characteristics
on the wake pressure distribution. It is felt that the inter-
actions are somewhat complicated, particularly in view of the
projection of the cargo doors, and other irregular geometry.
It is suggested that this wake flow be investigated in wind
tunnel tests where the power effects are included.

IV. REFERENCES

1.   Lockheed Drawing No. 3M08002, Sales Model C141A, 2/6/62.

2.   J. W. Pieper, et al: C-141A Engineering Flight Test Results of the Aerial Delivery System Tests, AD 633 249, Lockheed-Georgia Company, February 11, 1966.

3.   Herbert S. Ribner: Field of Flow About a Jet and Effect of Jets on Stability of Jet-Propelled Airplanes, NACA ACR No. L6C13.
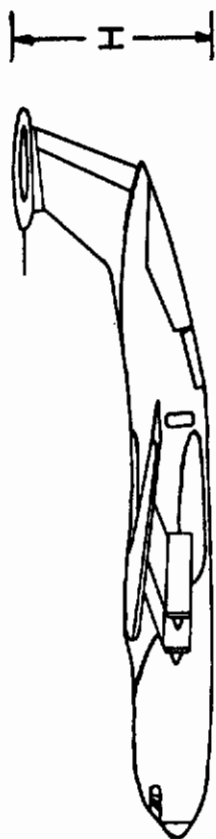
KEY
L = 1736 in (1/56 : 31 in)
H = 452 in (1/56 : 8 in)
S̄ = 1900 in (1/56 : 34 in)

Fig 1   Lockheed C-141A Jet Transport

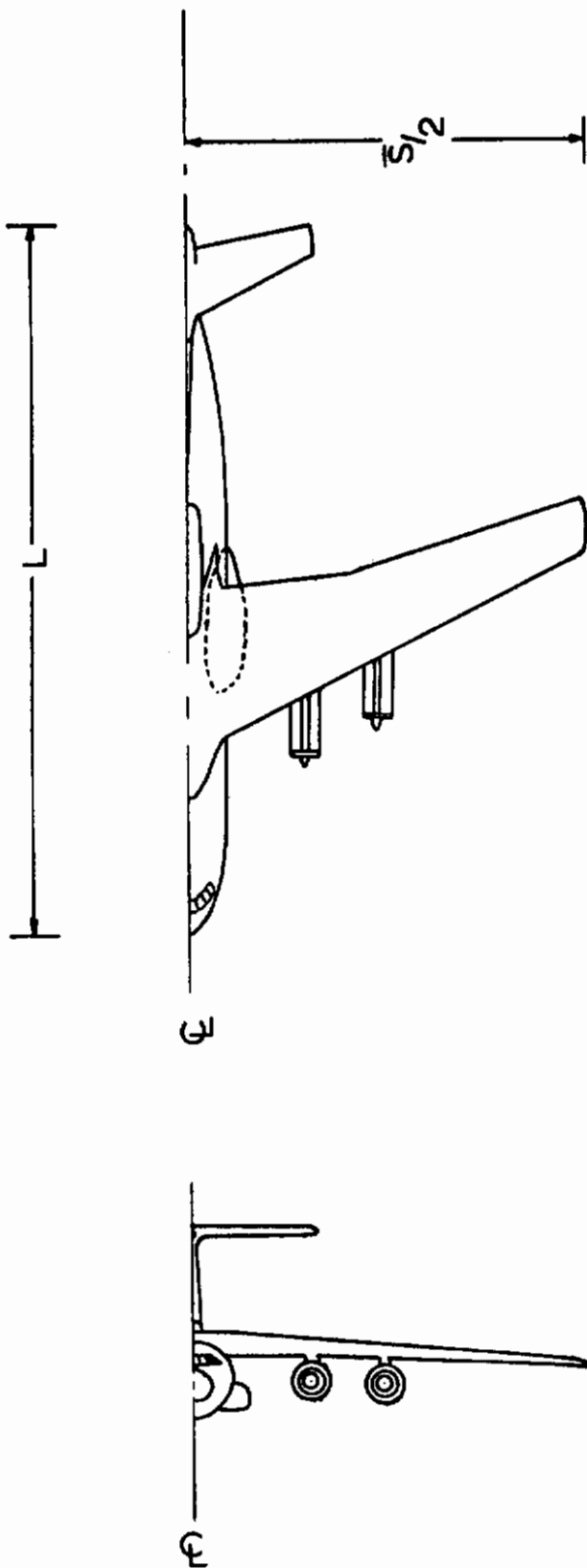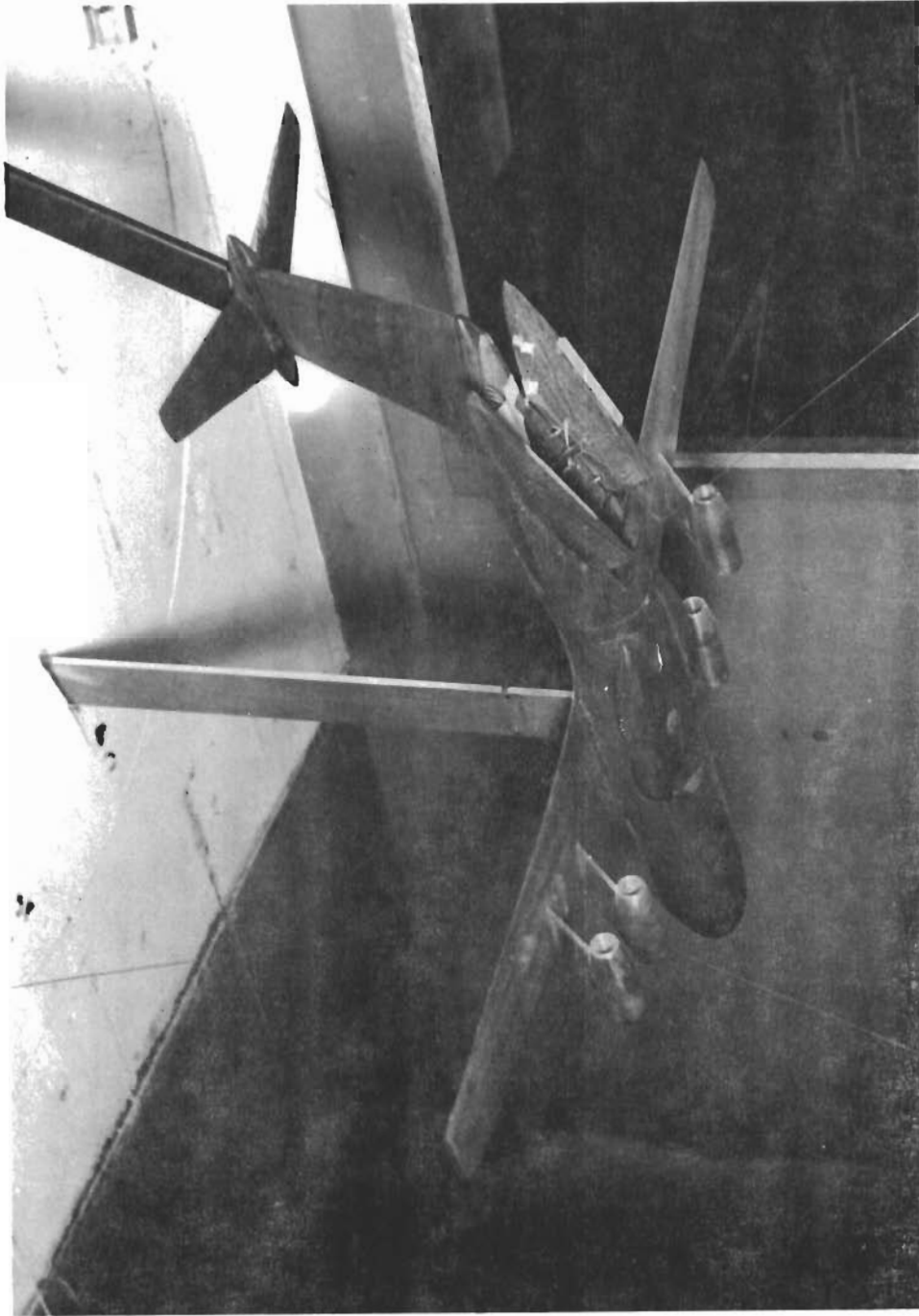Fig 2   Open-door Configuration for Surface   Pressure
Measurements in Wind Tunnel
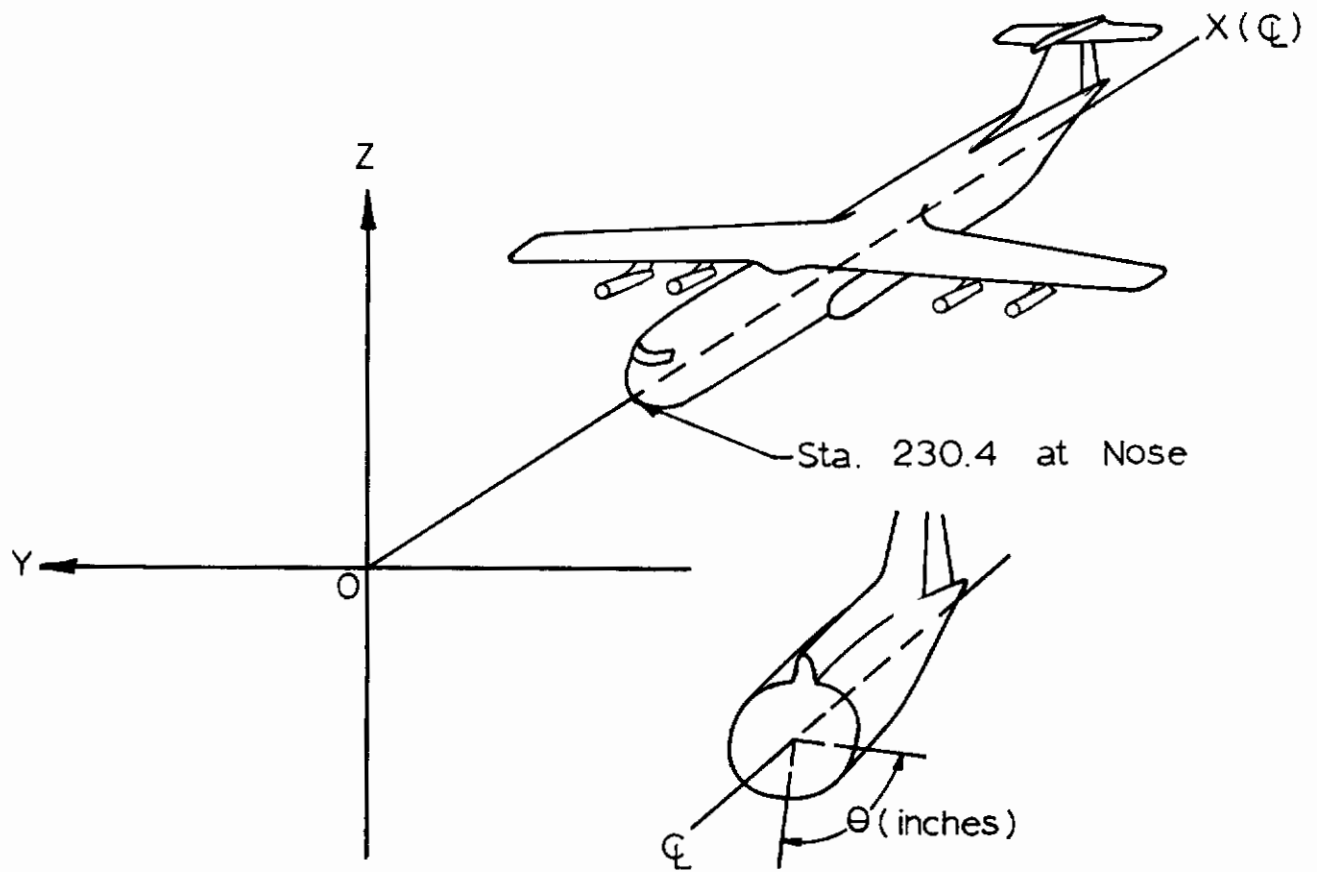
Fig 3   Coordinate   System   for   C-141A
         Data   Presentation   (Ref. 1)
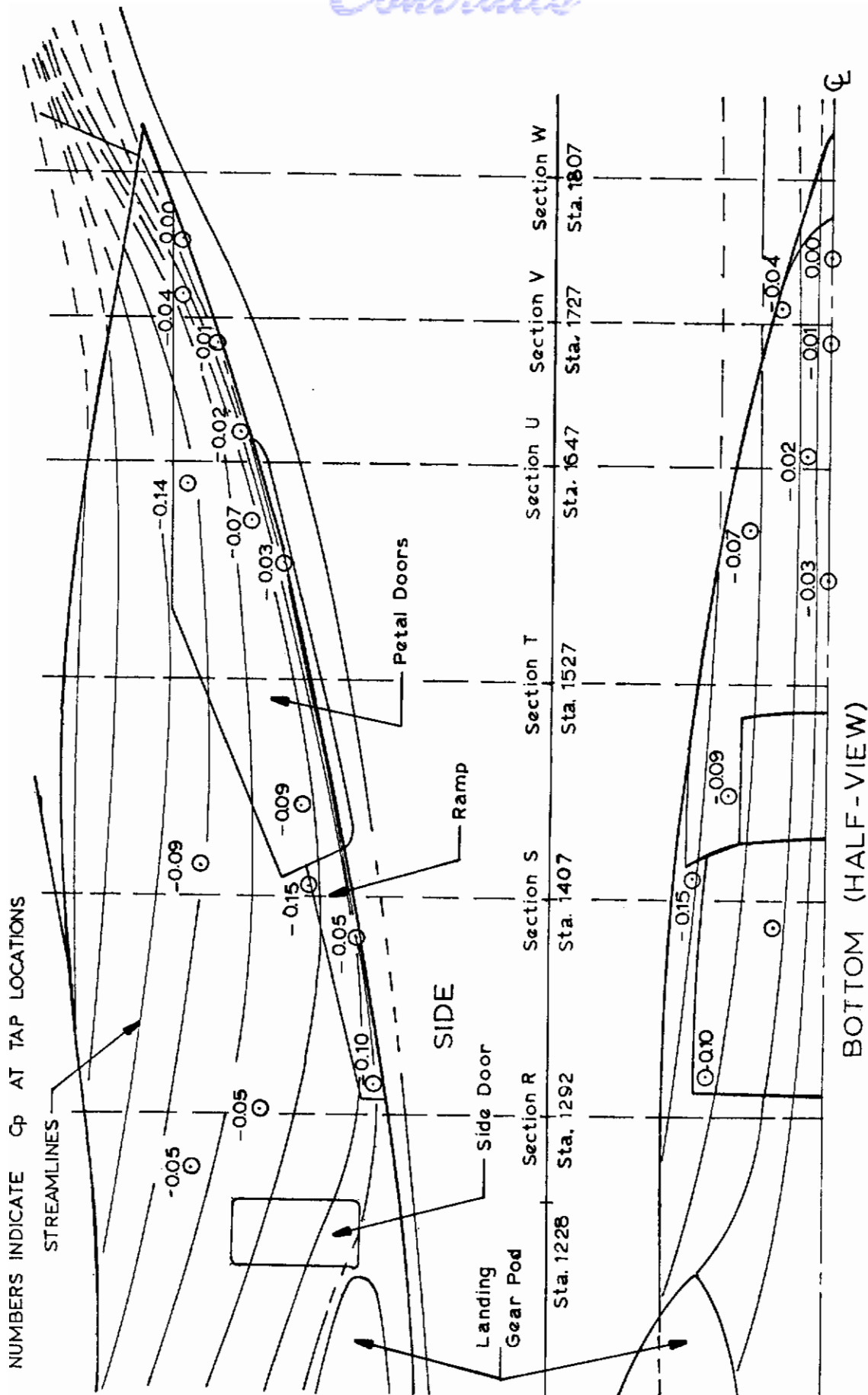
Fig 4   Stern of C-141A Model (Doors Closed) Showing Streamline Pattern and Pressure Coefficients
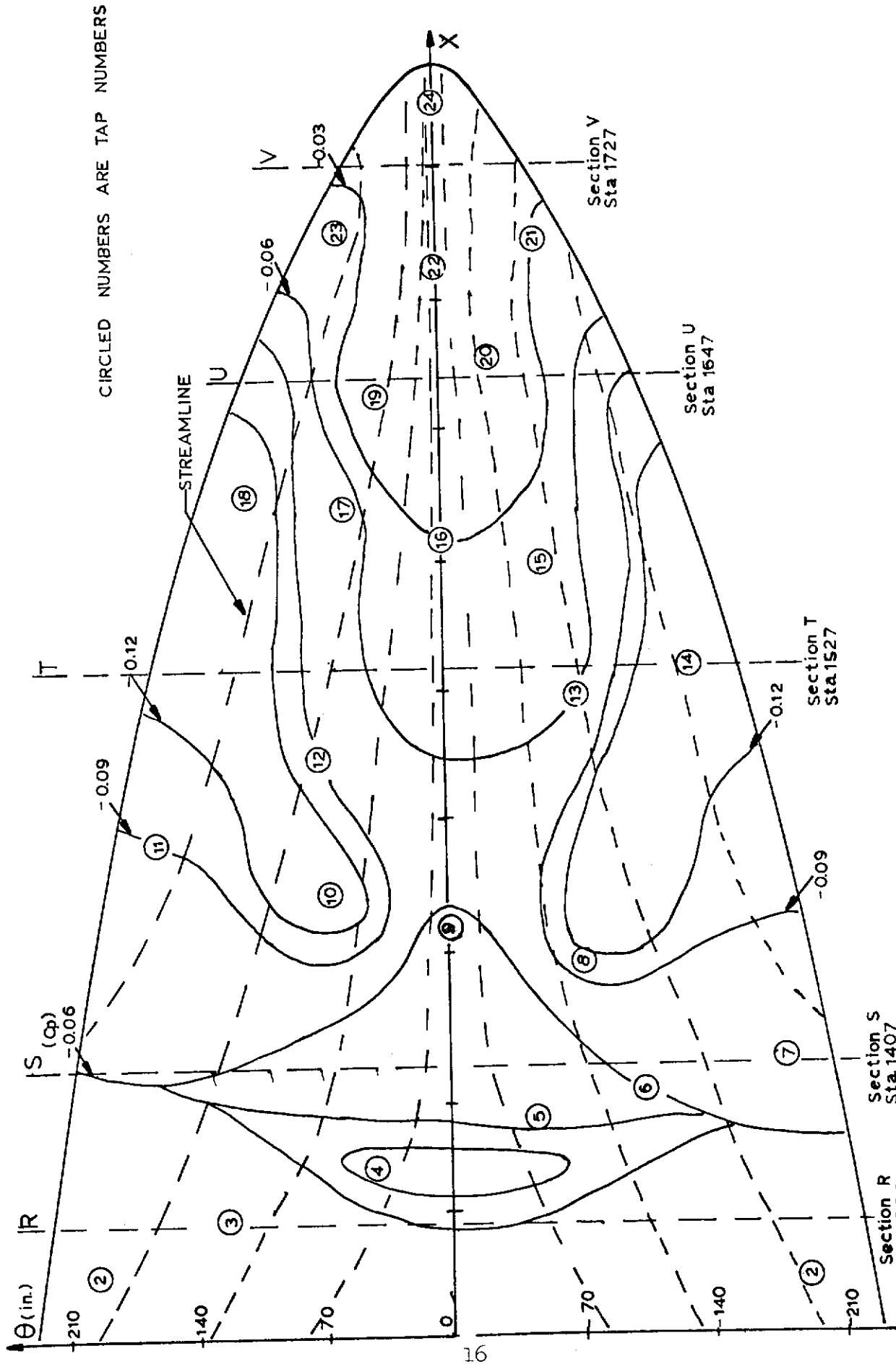
Fig 5 Mercator Projection of Stern Surface with Doors Closed Showing Pressure Distribution and Streamlines (Table I)

SECTION   R
Sta. 1292

0.05

0.05

$C_p = 0.06$

SECTION   S
Sta. 1407

0.06

PETAL
DOOR EDGE

0.05

$C_p = 0.04$

Sta. 1507
SECTION T

PETAL DOOR
EDGE

0.12

0.09

0.06

$C_p = 0.04$

Sta. 1647
SECTION U

PETAL DOOR
EDGE

0.09

0.06

$C_p = 0.03$
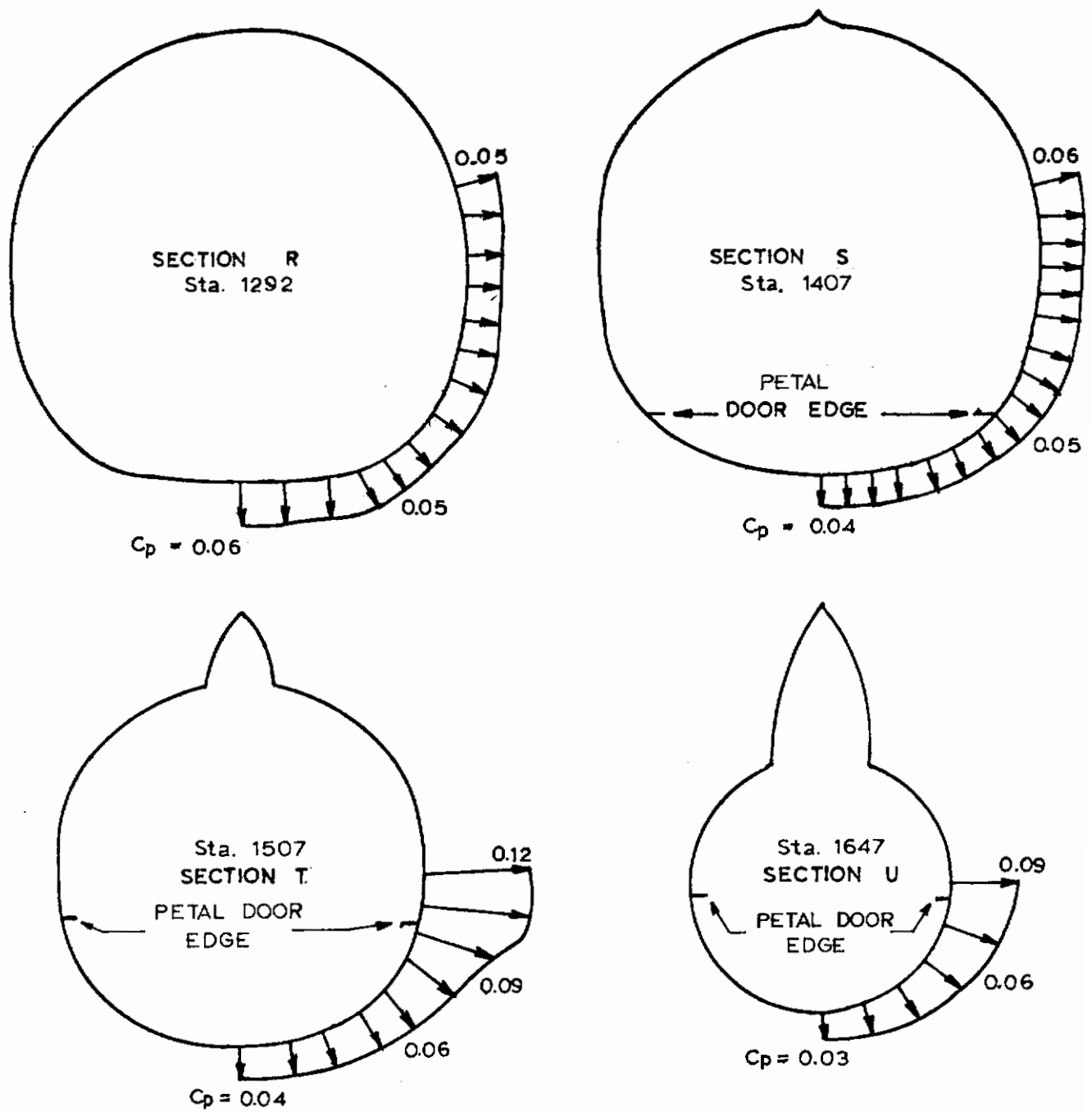
Fig 6   Pressure   Distribution   about   Cross
Sections* R , S, T, and U with Doors
Closed
*Ref. 1

17
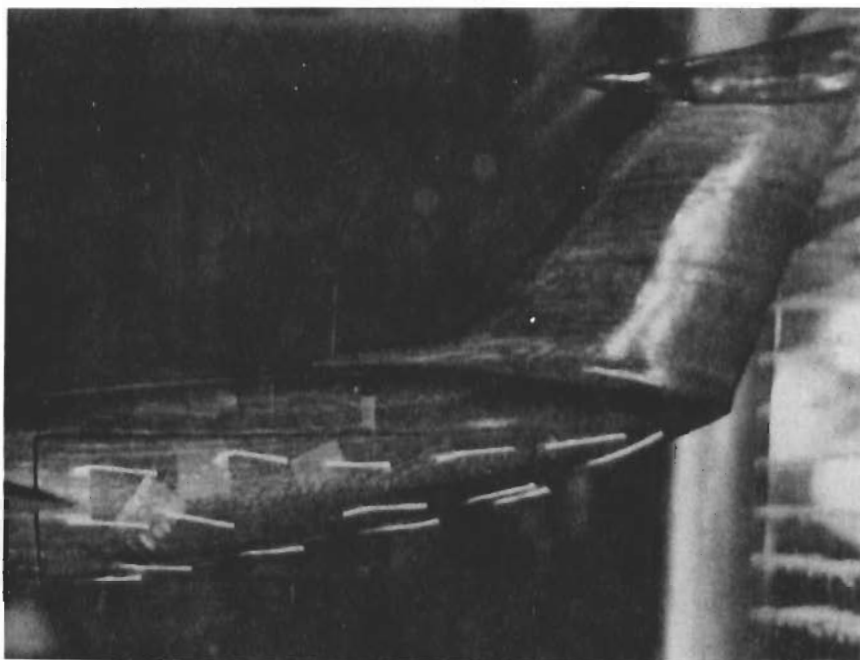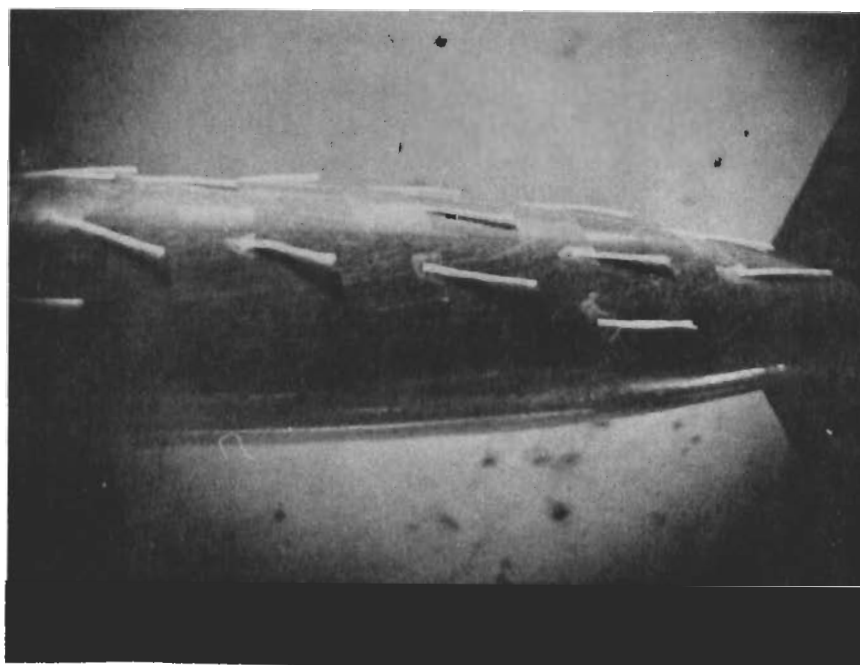
SIDE

BOTTOM

Fig 7   Simultaneous Side and Bottom Views of
Tufted Stern with Doors Closed (V_∞ = 200fps)
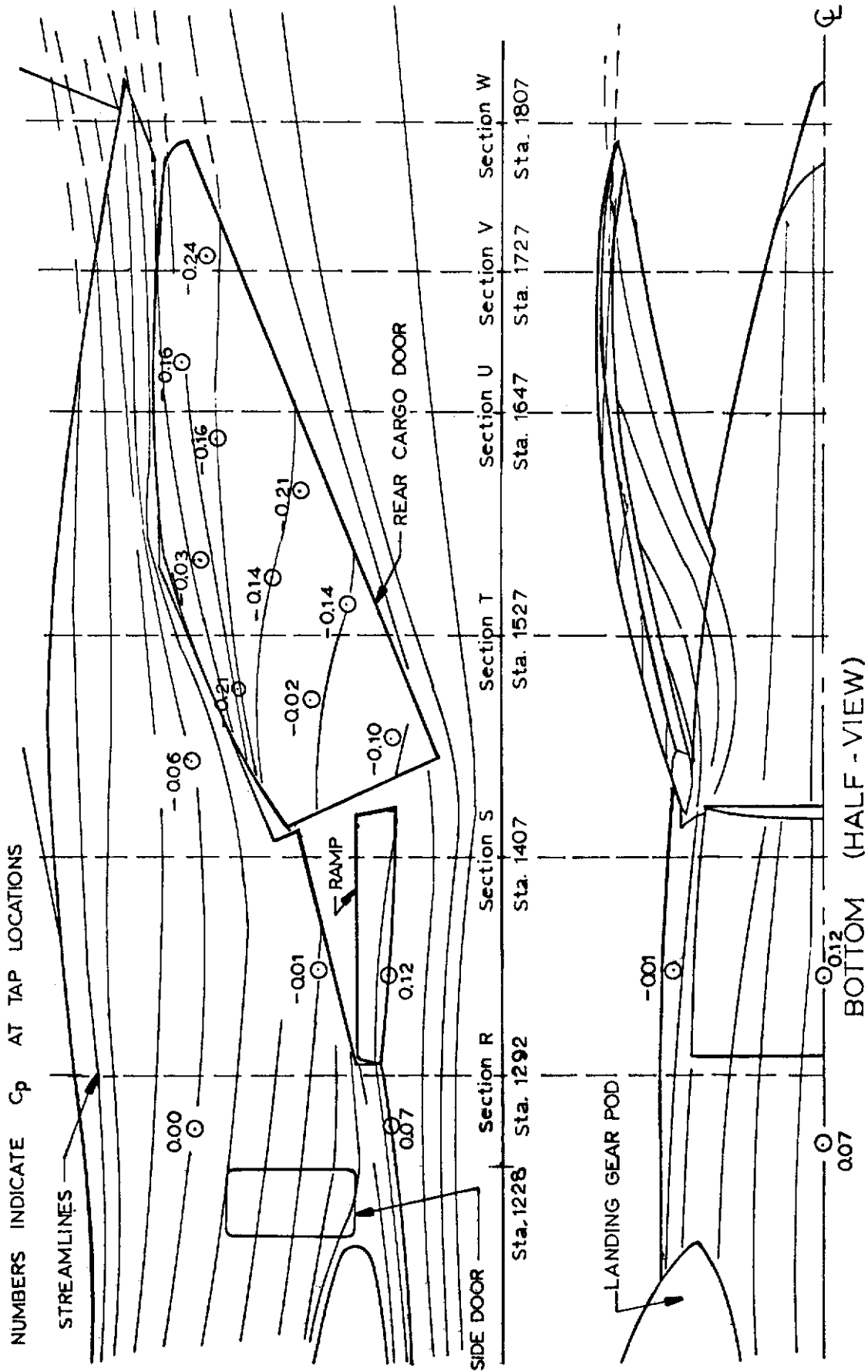
Fig 8 Stern of C-141A Model (Doors Open) Showing Streamline Pattern and Pressure Coefficients

19
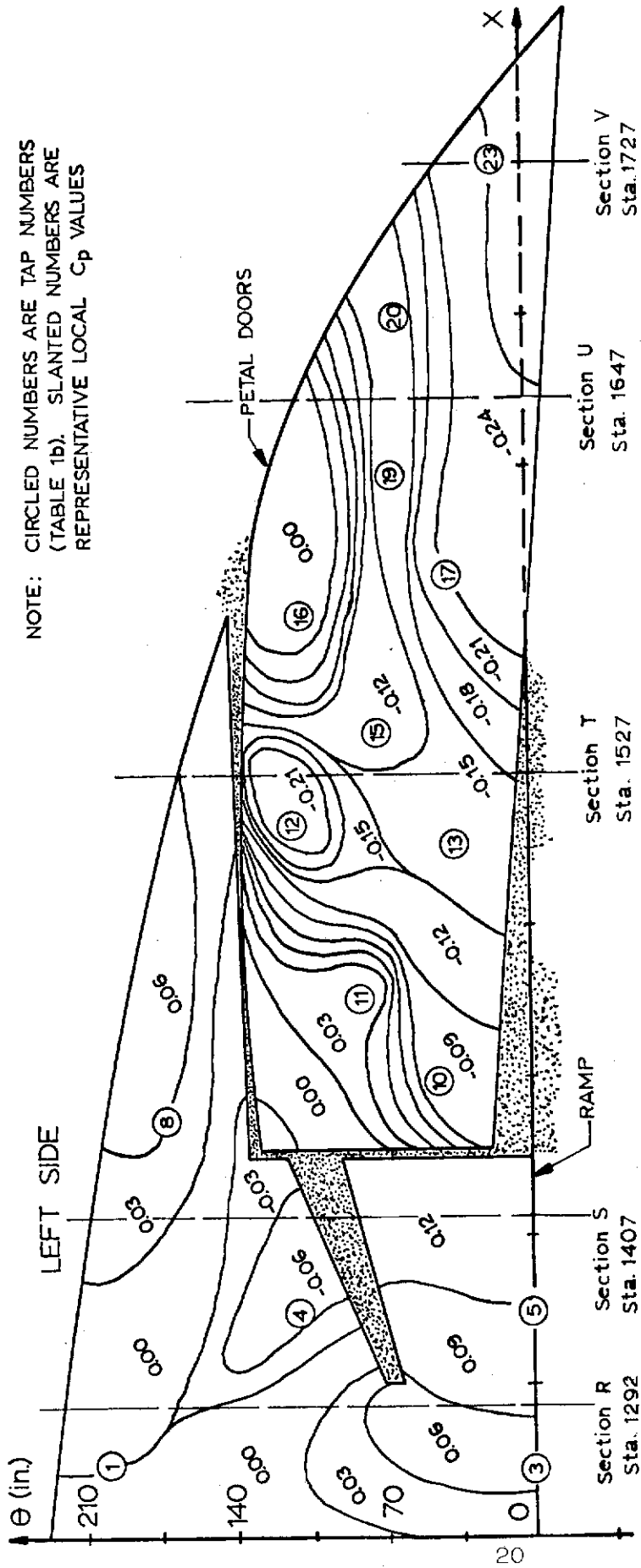
Fig 9   Half-view Mercator Projection of Stern Surface with Doors Open Showing Pressure Distribution (Table I)
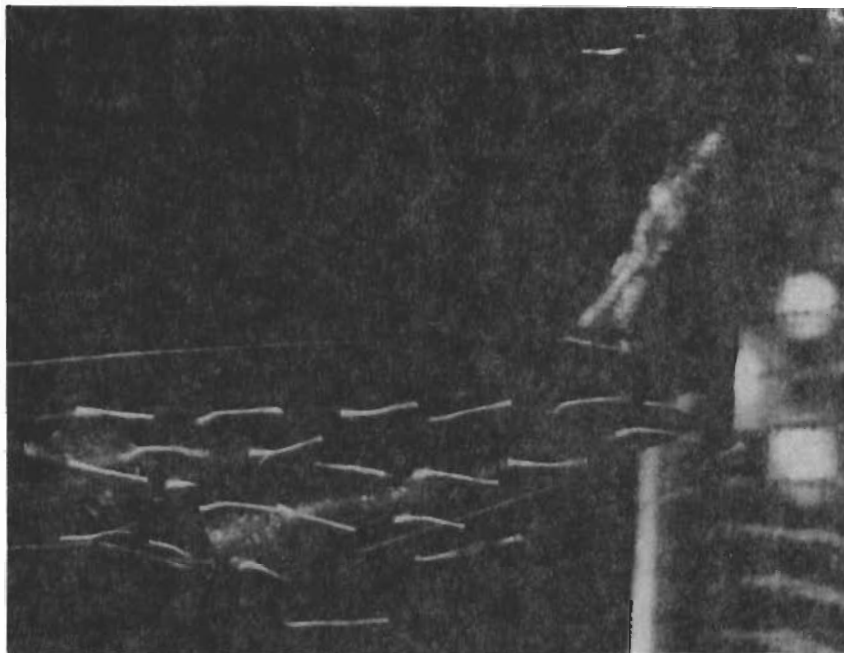
SIDE
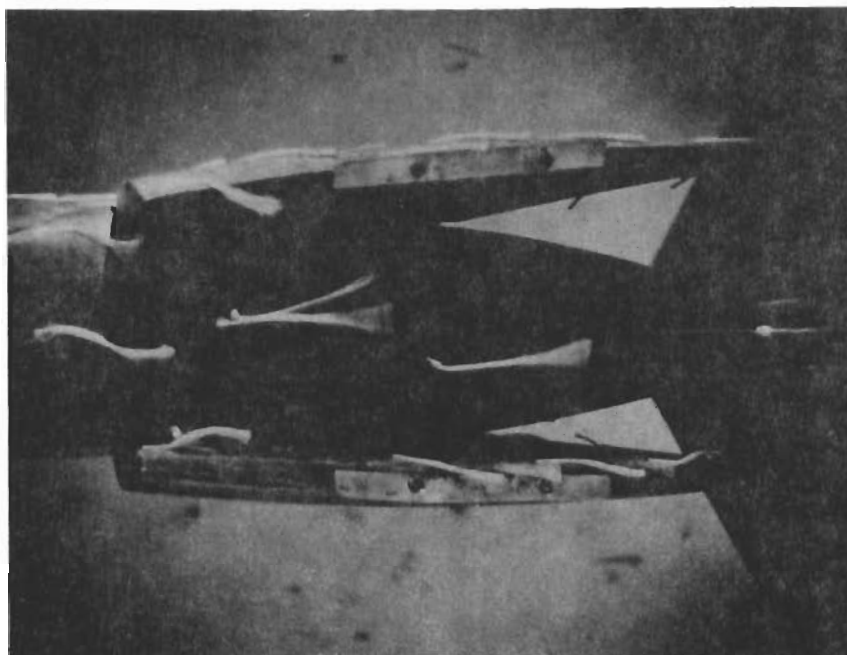
BOTTOM

Fig 10 Simultaneous Side and Bottom Views of Tufted Stern with Doors Open 65° ($V_\infty \doteq 200$ fps)

21
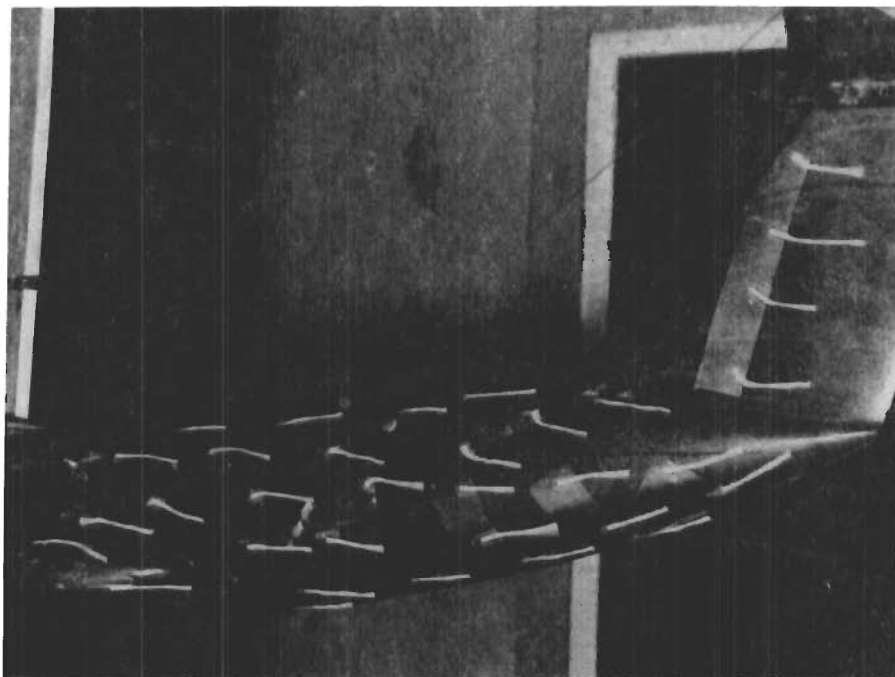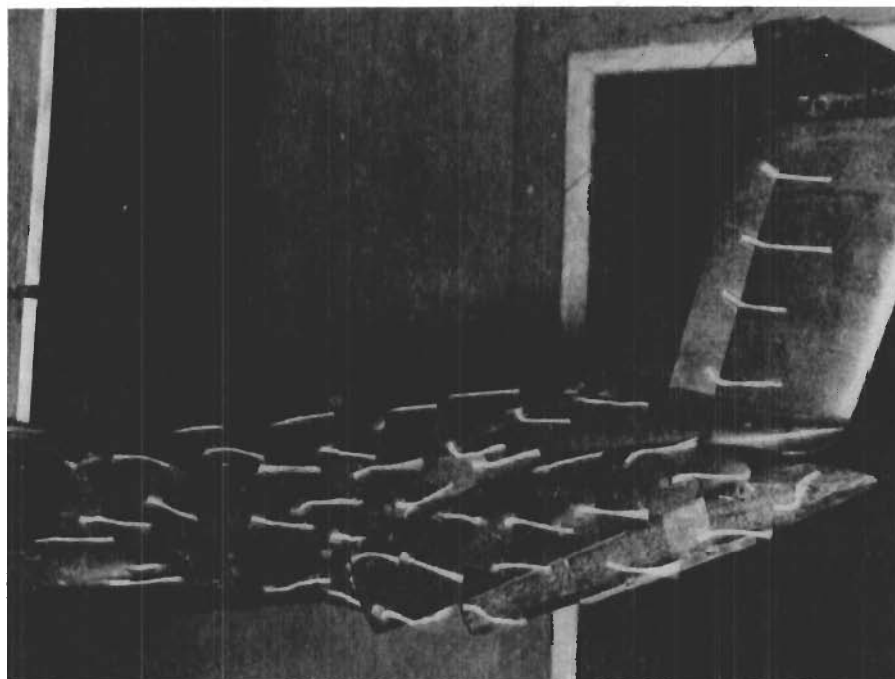
DOORS CLOSED

DOORS OPENED 65°

Fig 11 Comparative Views of Tail Sections with Doors Closed and Open ($V_\infty \doteq 230$ fps)

22

1.315" long

1.0" long

1.0' (0.10 ea)

2.5" (0.25 ea)

3.0" (0.75 ea)

15.0"

NOTE: RAKE HAS
ALTERNATING TOTAL
AND STATIC
PRESSURE PROBES,
DIAM.= 0.035"
TAP DIAM.= 0.035"
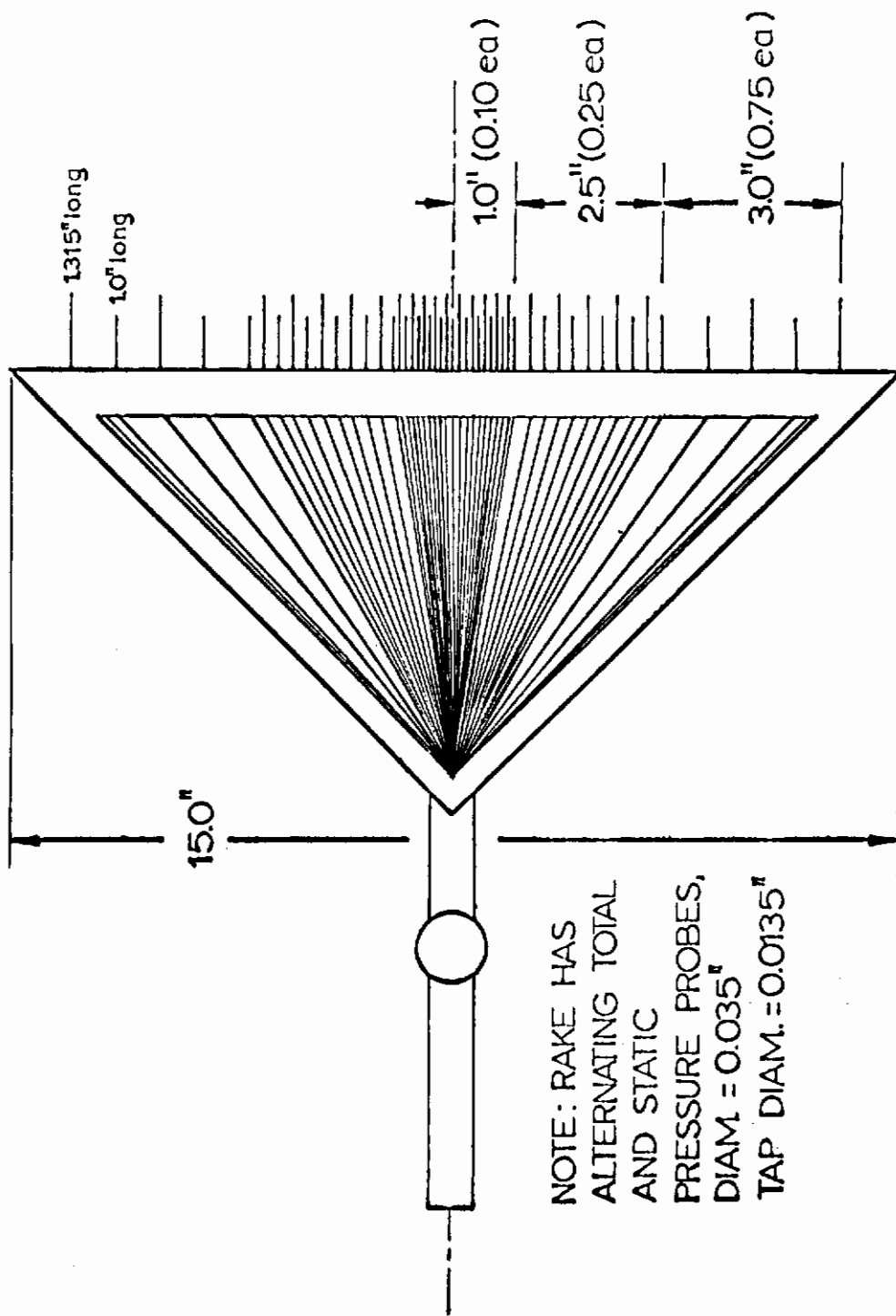
Fig 12   Pressure   Survey   Rake

approximate size and position
of a 22ft. extraction para-
chute attached at A/C C.G.
with standard 140ft. ex-
traction line.
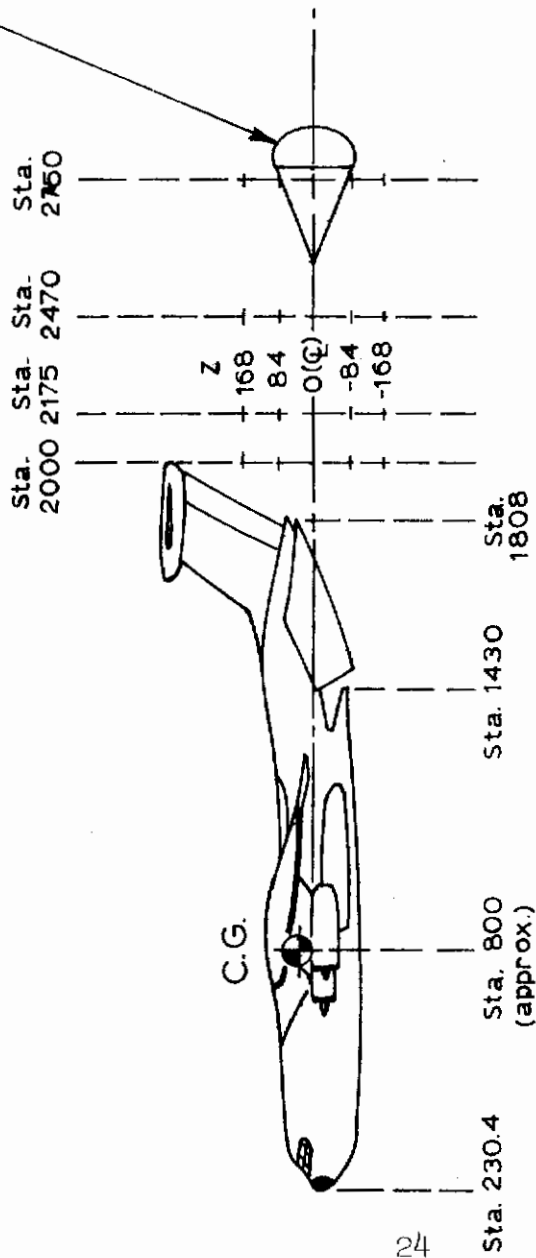
note: all dimensions and
station numbers
are inches and
refer to full
scale.

Sta. 230.4

Sta. 800
(approx.)

C.G.

Sta. 1430

Sta.
1808

Sta.
2000

Sta.
2175

Sta.
2470

Sta.
2750

Z
168
84
O(℄)
-84
-168

24

Fig 13 Positions of Wake Survey Rake
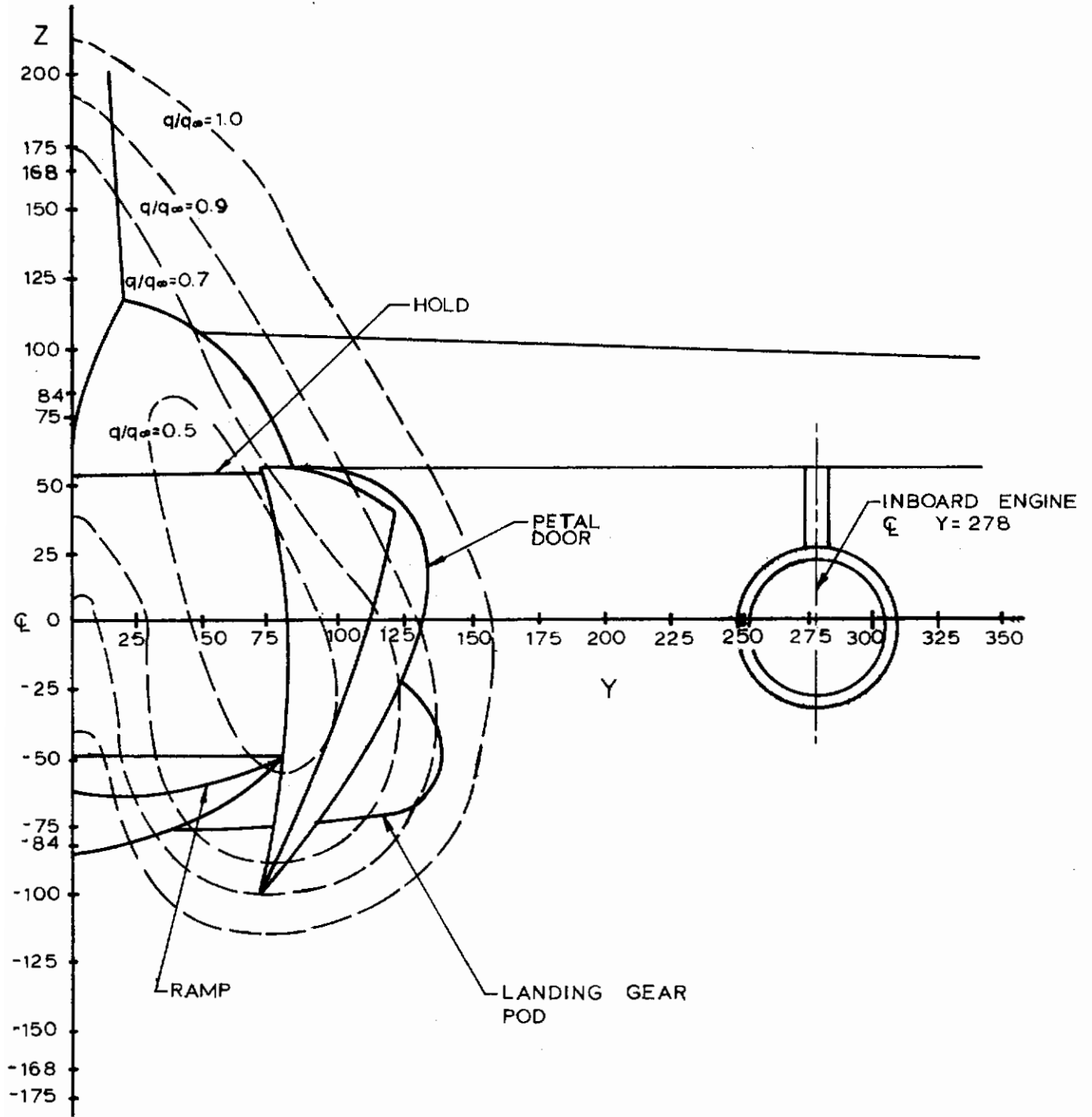
Fig 14   Pressure Contour Lines in
Wake of C-141A at Station 2000
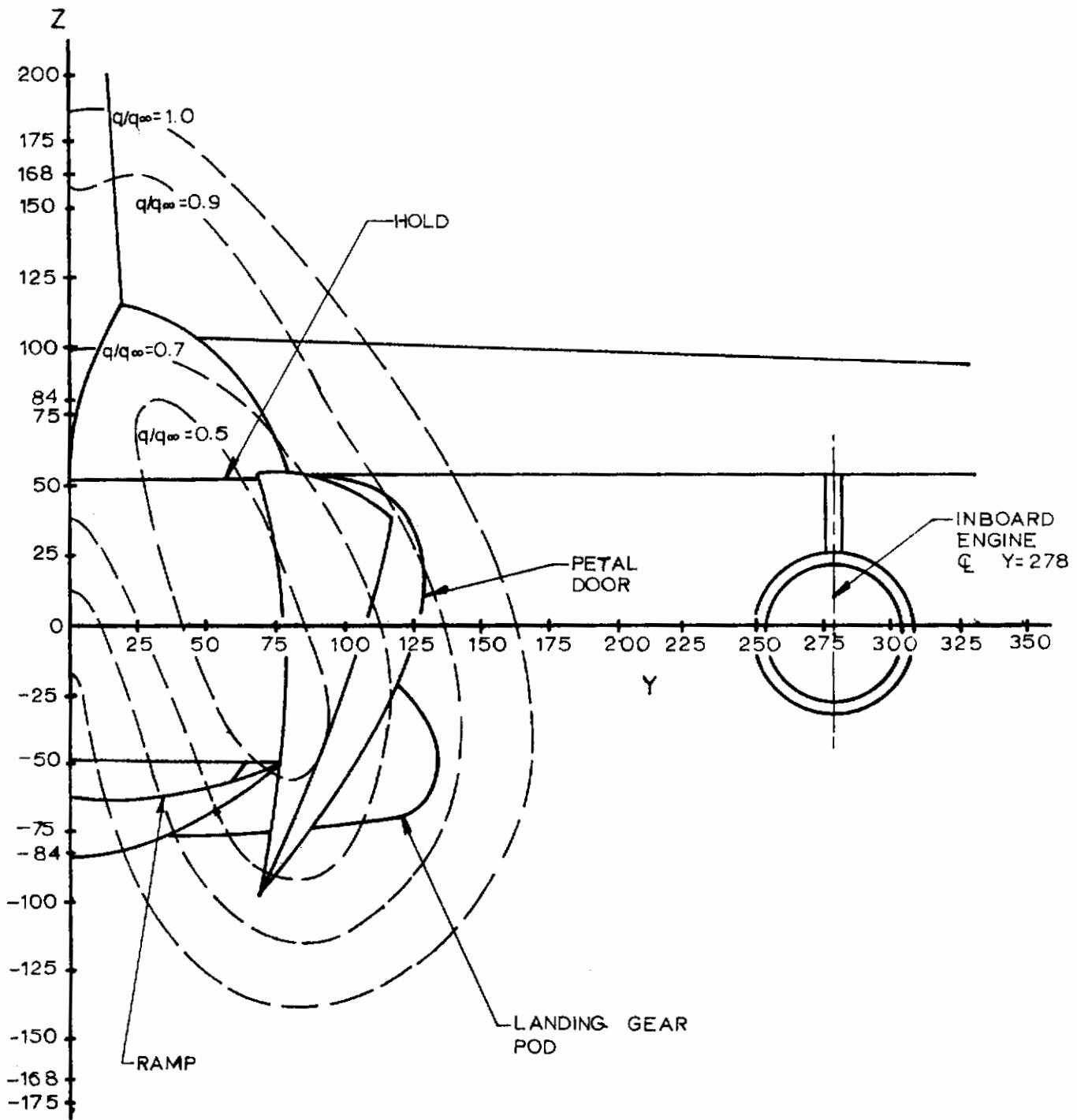
Fig 15   Pressure Contour Lines in
Wake of C-141A at Station 2175

26

Fig 16   Pressure Contour Lines in
Wake of C-141A at Station 2470

Contrails

Z

200

175
168

150

125

100

84
75

50

25

₵   0

-25

-50

-75

-100

-125

-150

-168
-175

$q/q_\infty=1.0$

$q/q_\infty=0.9$

$q/q_\infty=0.7$

HOLD

INBOARD ENGINE ₵ Y=278

PETAL DOOR

25 50 75 100 125 150 175 200 225 250 275 300 325 350

Y

LANDING GEAR POD

RAMP
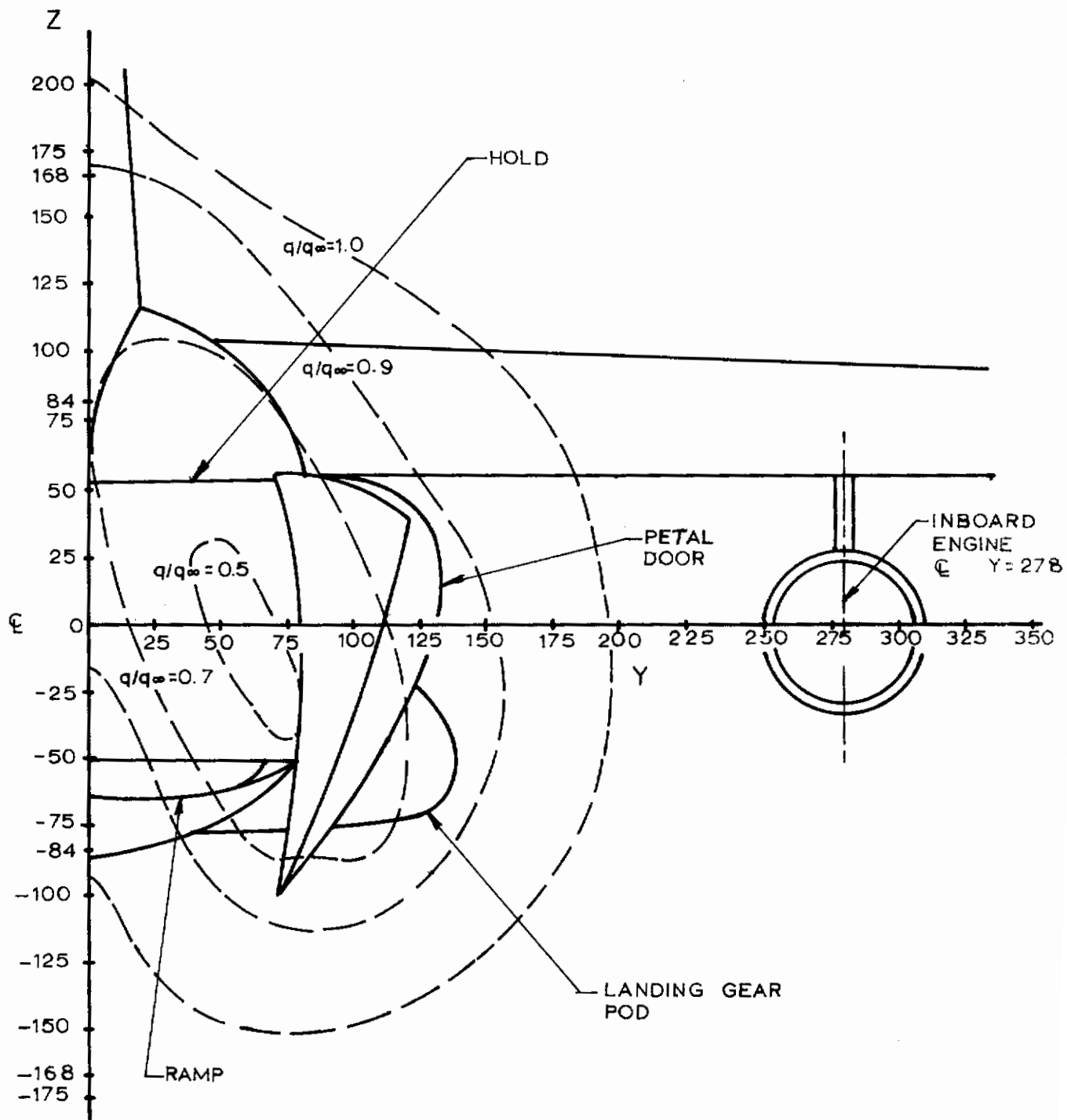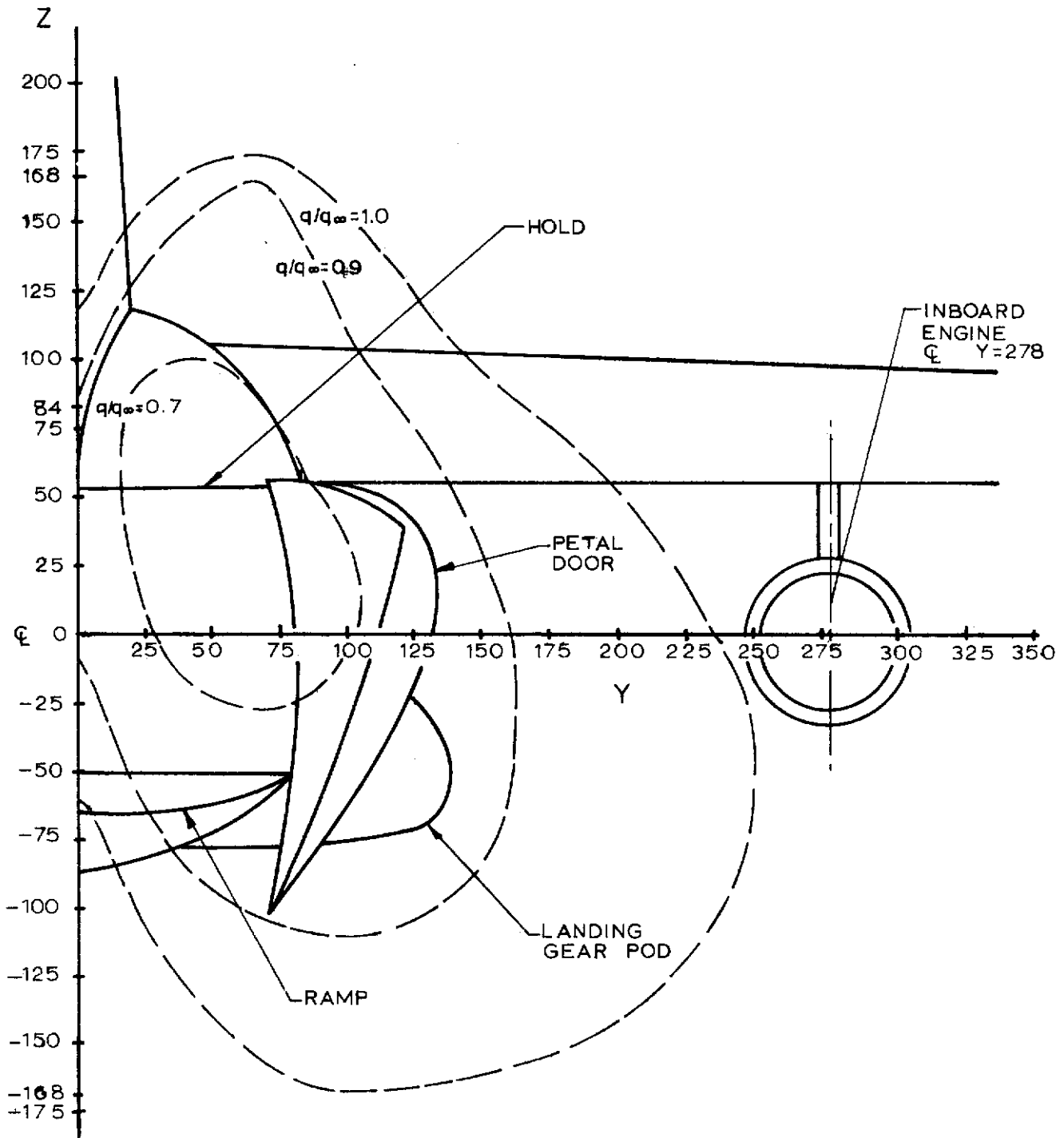
Fig 17   Pressure Contour Lines in
        Wake   of   C-141A   at   Station 2750
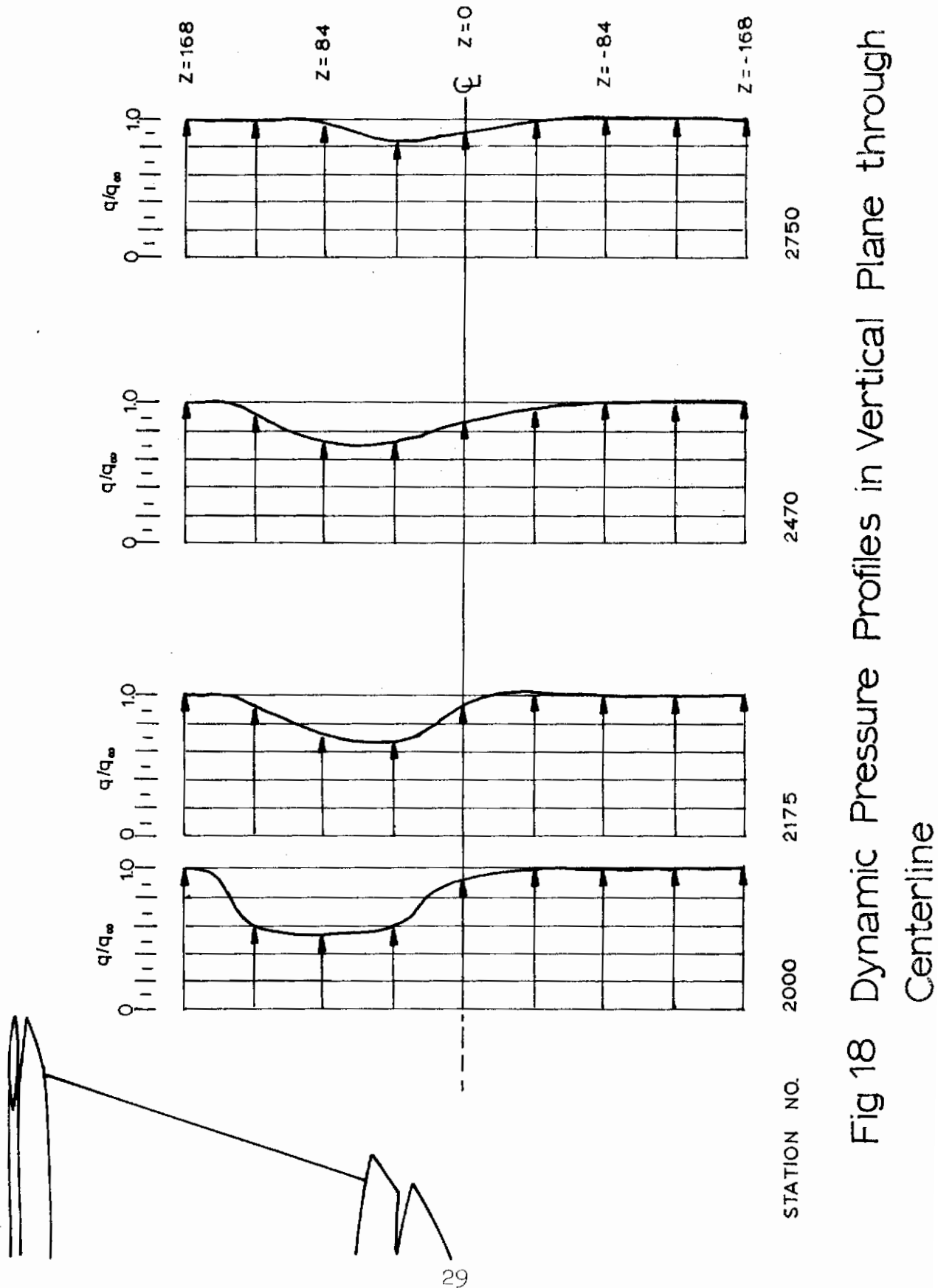
Fig 18   Dynamic Pressure Profiles in Vertical Plane through Centerline

STATION NO.   2000   2175   2470   2750
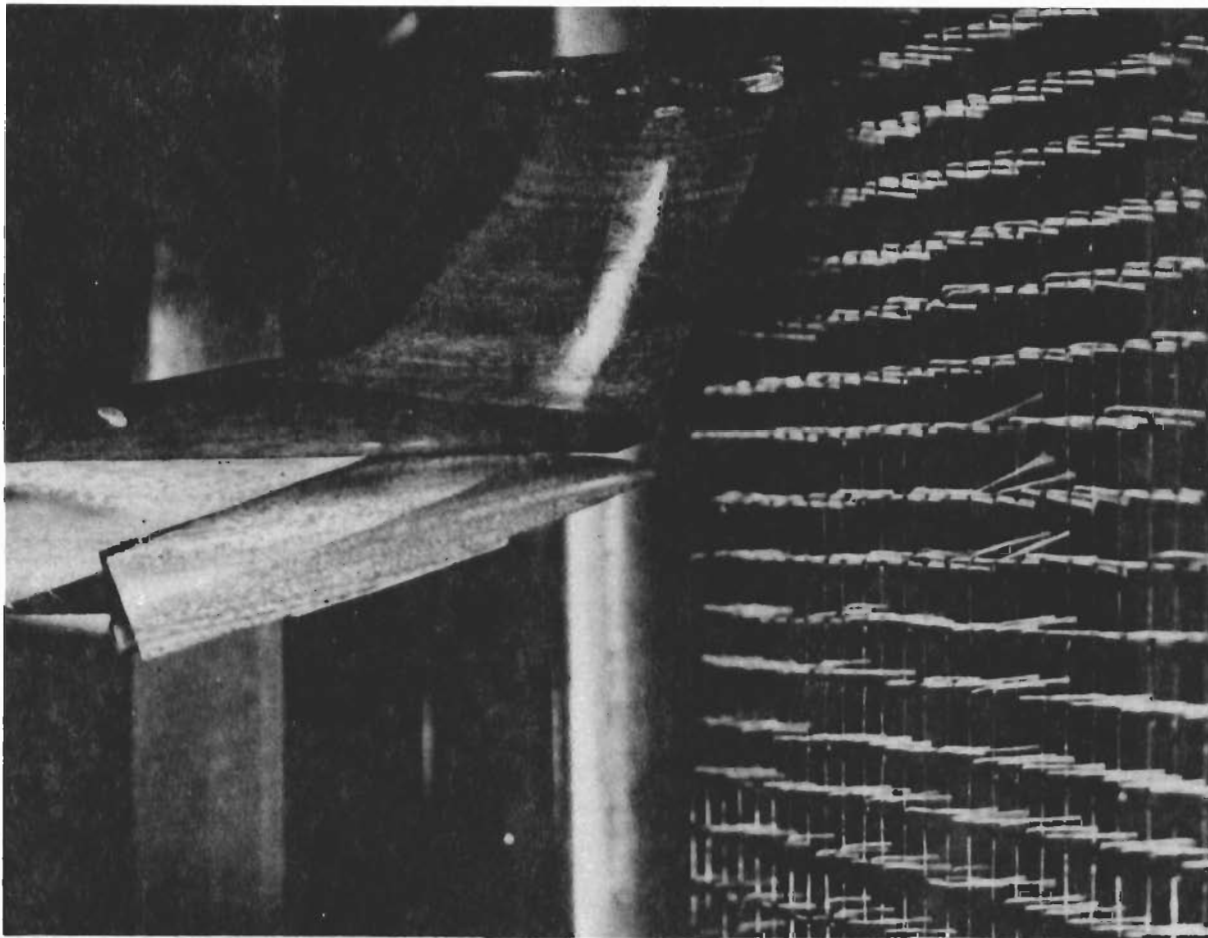
Fig 19   Tufted Grid at Tip of Horizontal
Stabilizer Showing Local Upwash
in Wake of Doors
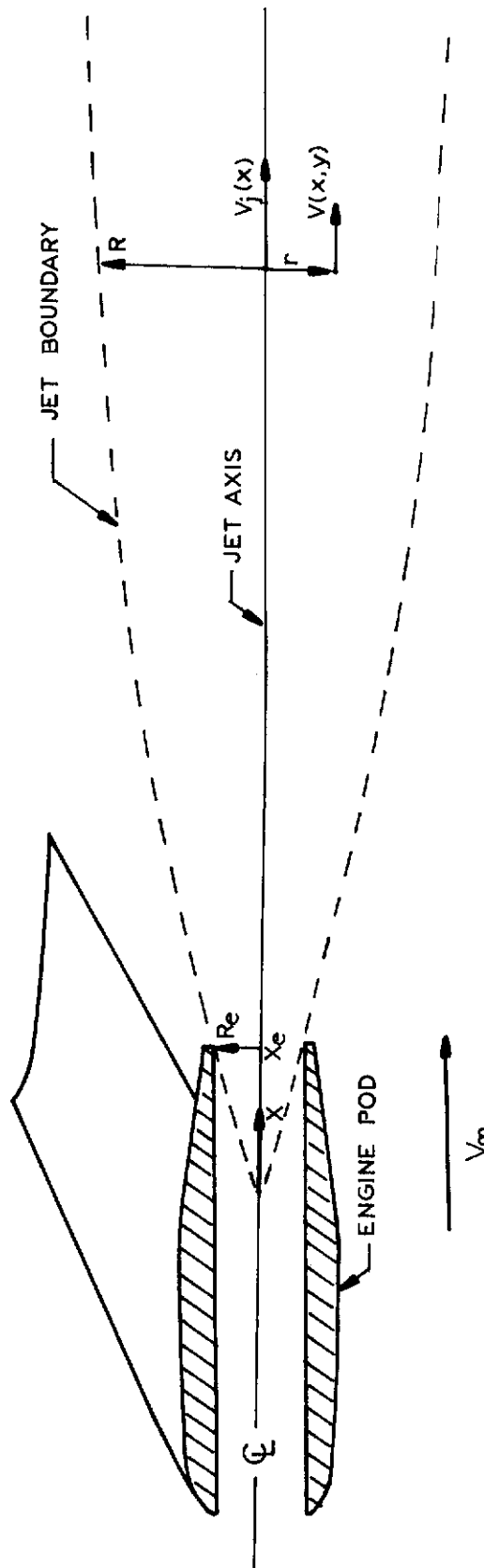
Fig 20 Coordinate System for Analytic Approximation
of Jet Effect on Wake (Ref 3)
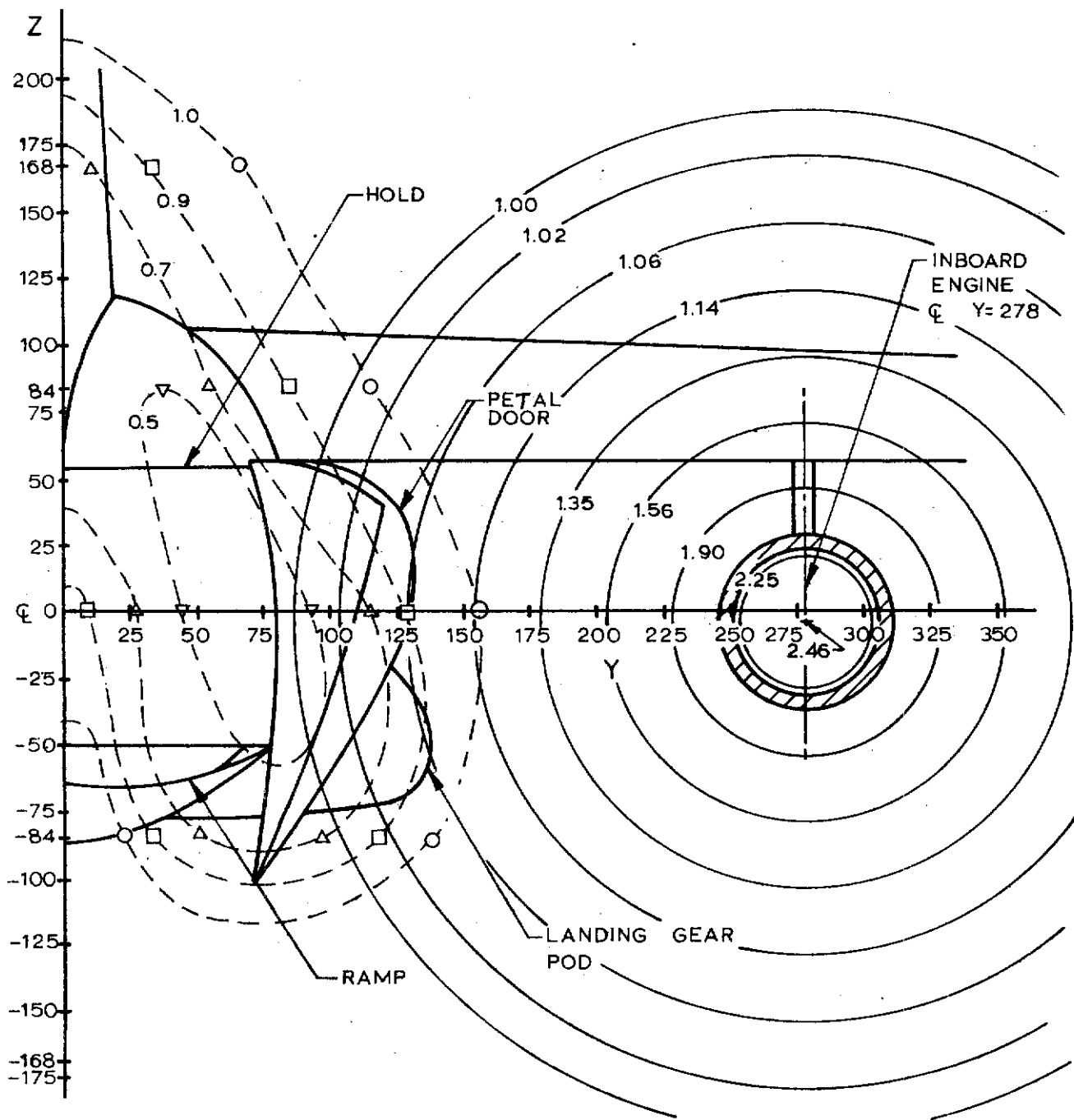
Fig 21 Pressure Contour Lines in
Wake of C-141A at Station 2000
with Power Effects
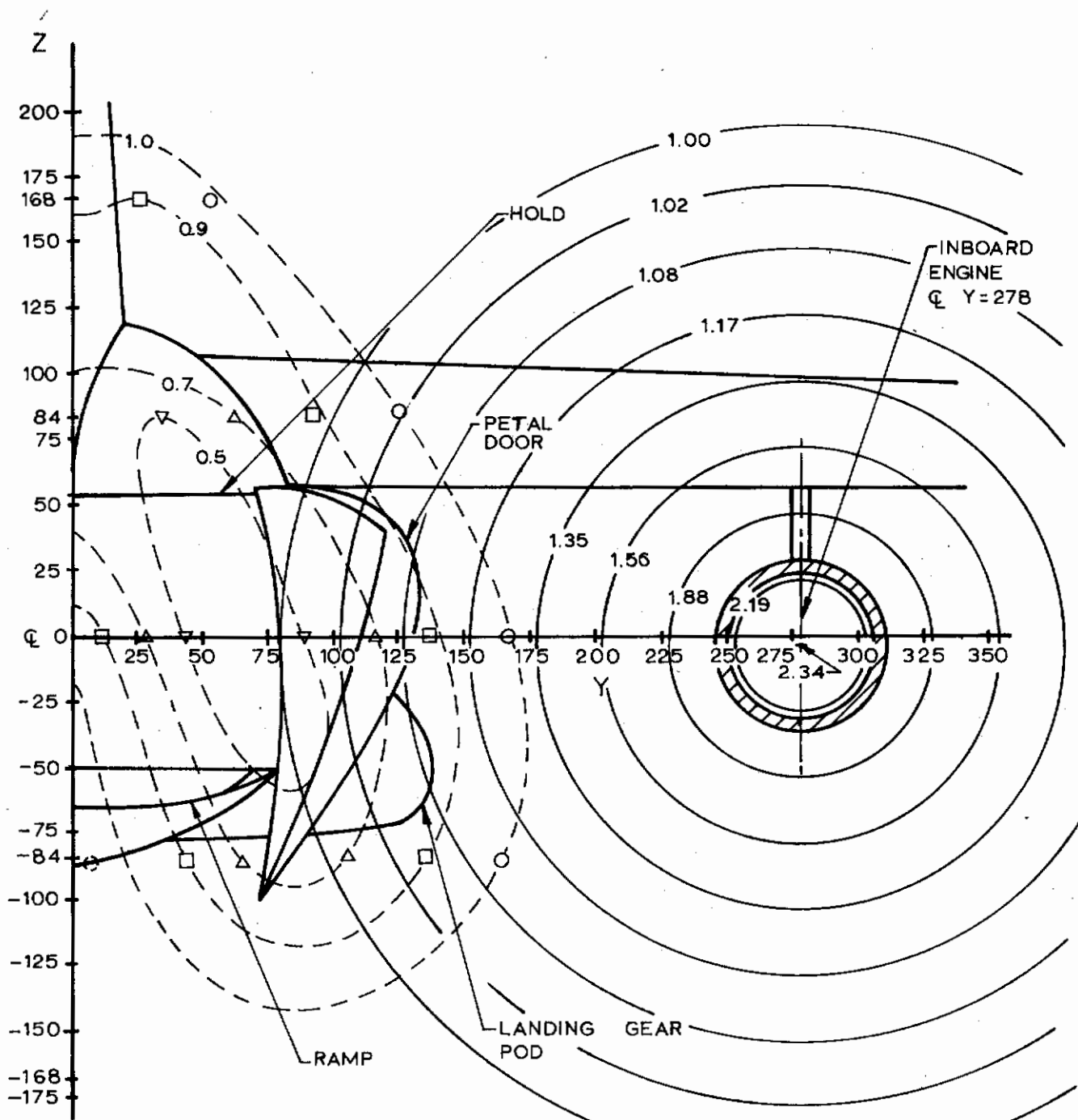
Fig 22   Pressure Contour Lines in
         Wake of C-141A at Station 2175
         with Power Effects

33
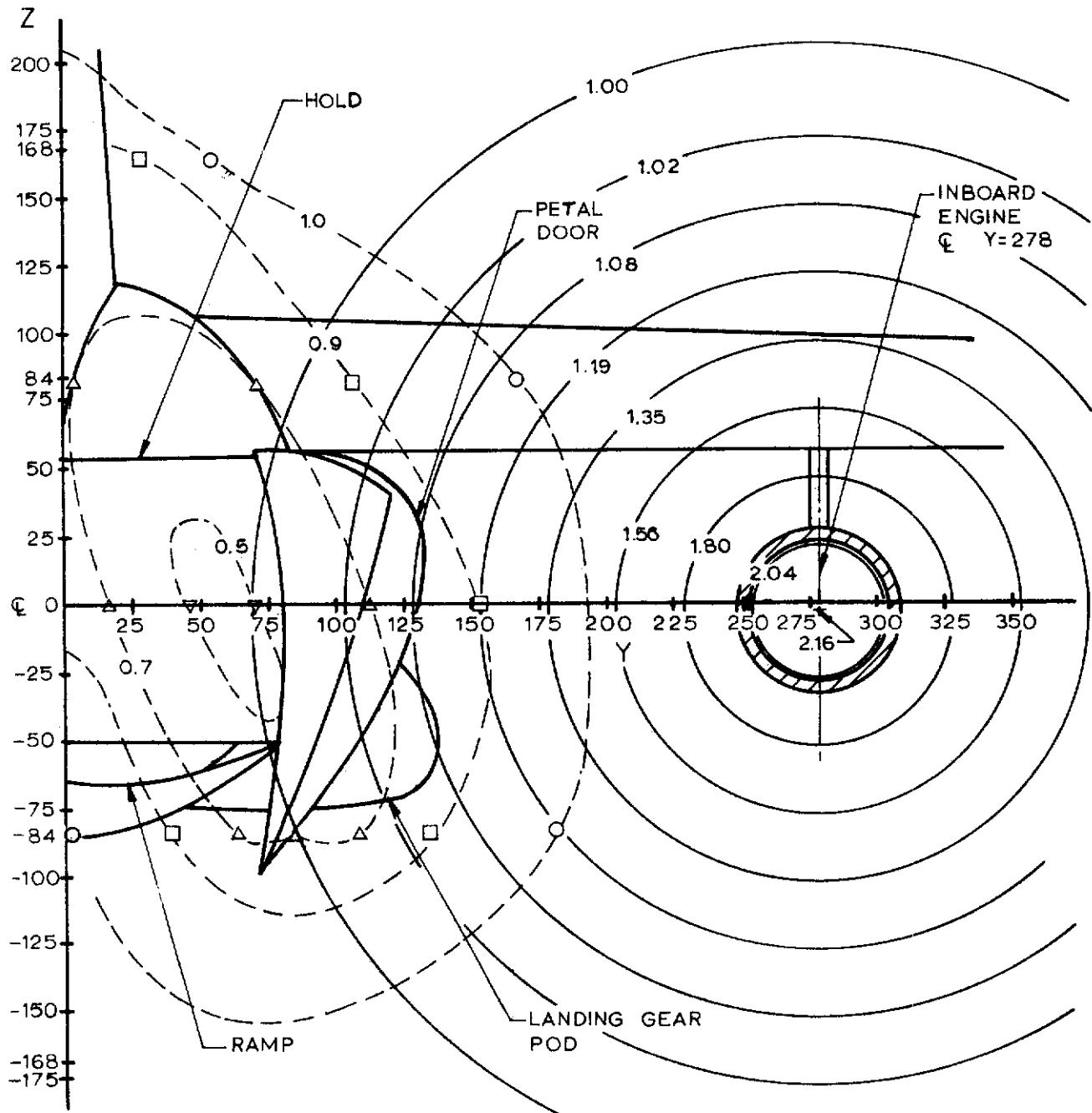
Fig 23   Pressure   Contour   Lines   in
Wake   of   C-141A   at   Station   2470
with   Power   Effects

34
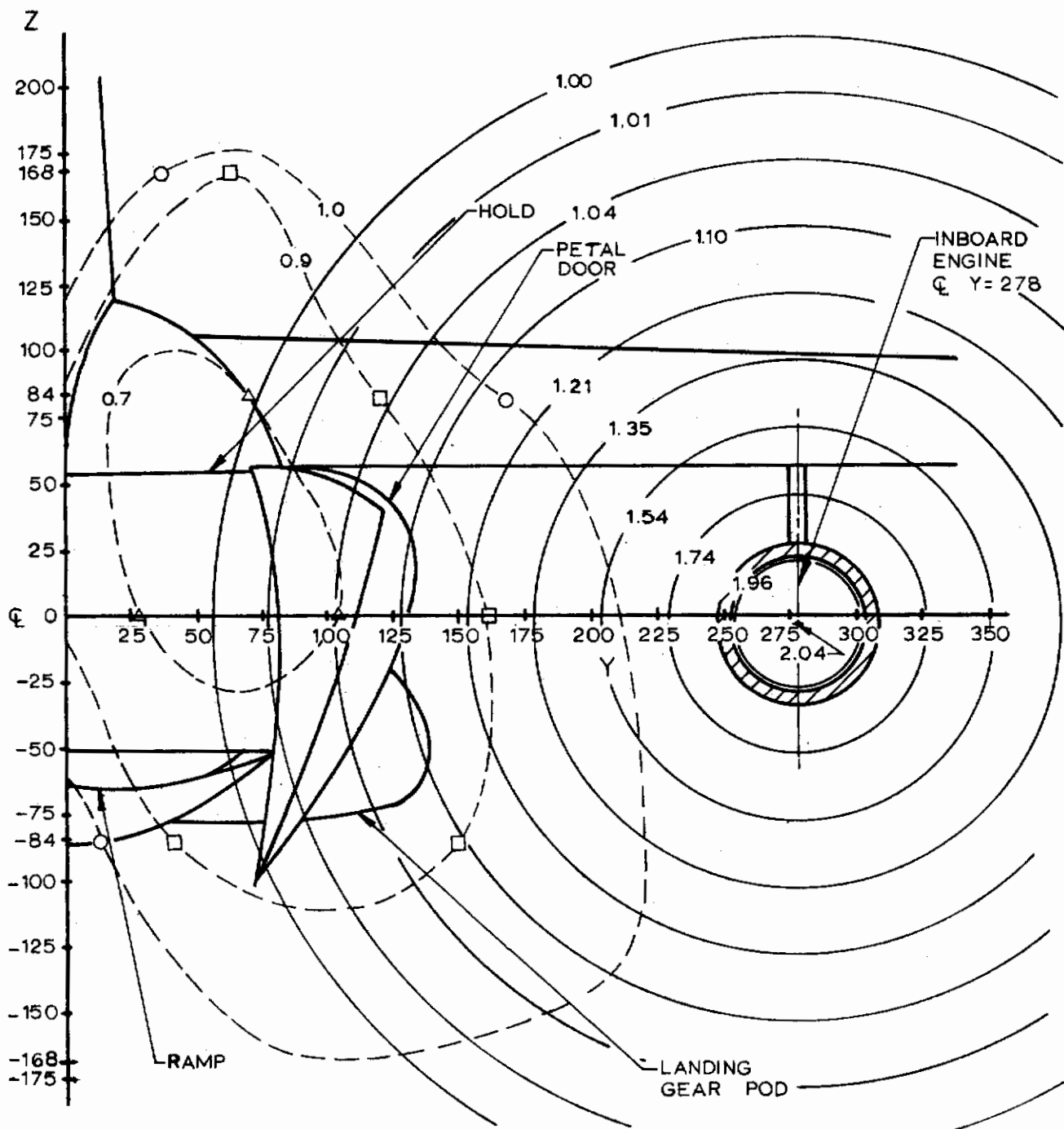
Fig 24   Pressure   Contour   Lines   in
      Wake   of   C-141A   at   Station   2750
      with   Power   Effects
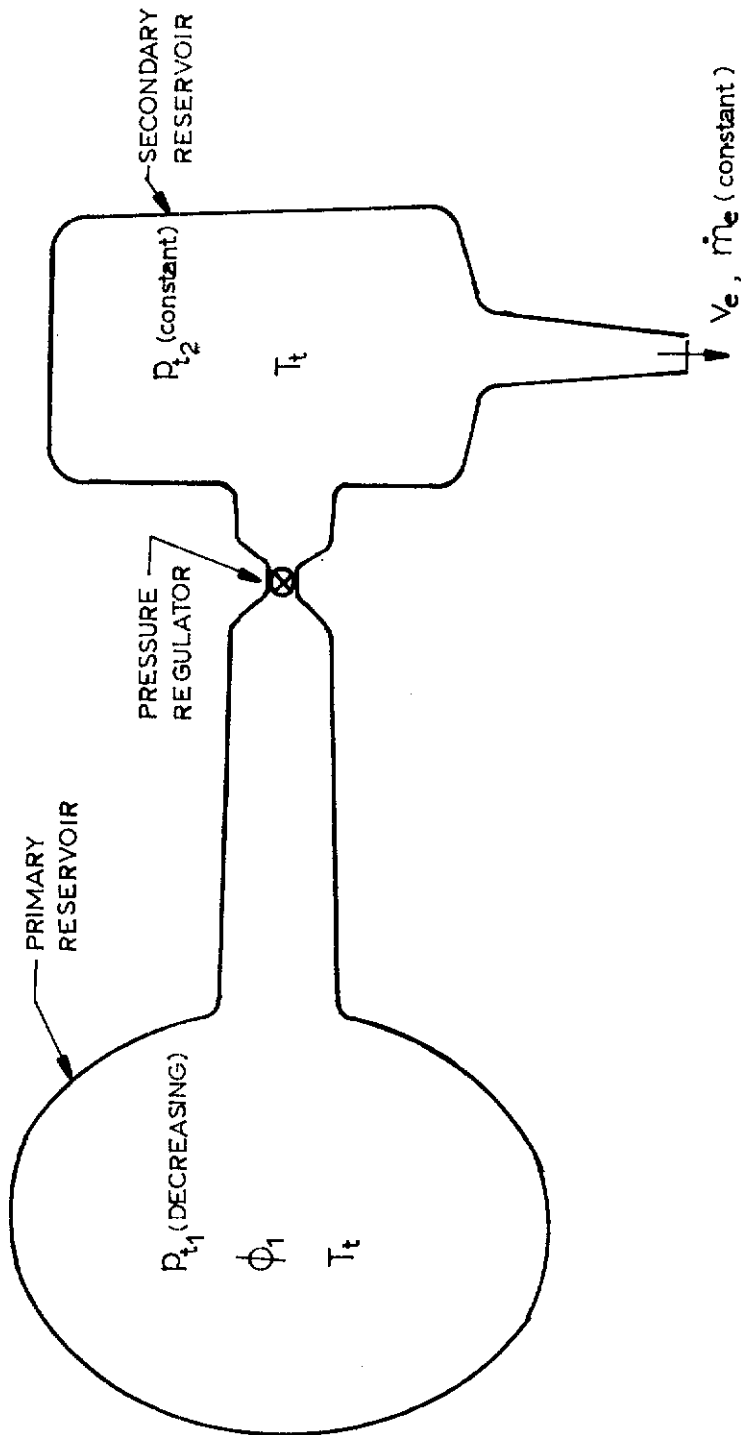
Fig 25 Schematic Diagram of Air Supply System for
Simulation of Engine Power

WIND TUNNEL WALL

$A_e = 0.00544 \text{ ft}^2 (0.5 \text{ in I.D.})$

PRESSURE RAKE

SUPPLY TUBES (1.00 in.O.D.)

20 in

7 ft

$P_{t_2} = 27 \text{ psi}$

SECONDARY RESERVOIR
(Max. thick. 1.5", Chord 10")

PRESSURE REGULATOR
(~30% pressure loss)

SUPPLY LINE
(~40% pressure loss)

PRIMARY
RESERVOIR

$P_{t_1} \le 127 \text{ psi}$

$\phi_1 = 140 \text{ ft}^3$

$T_t = 530°R$
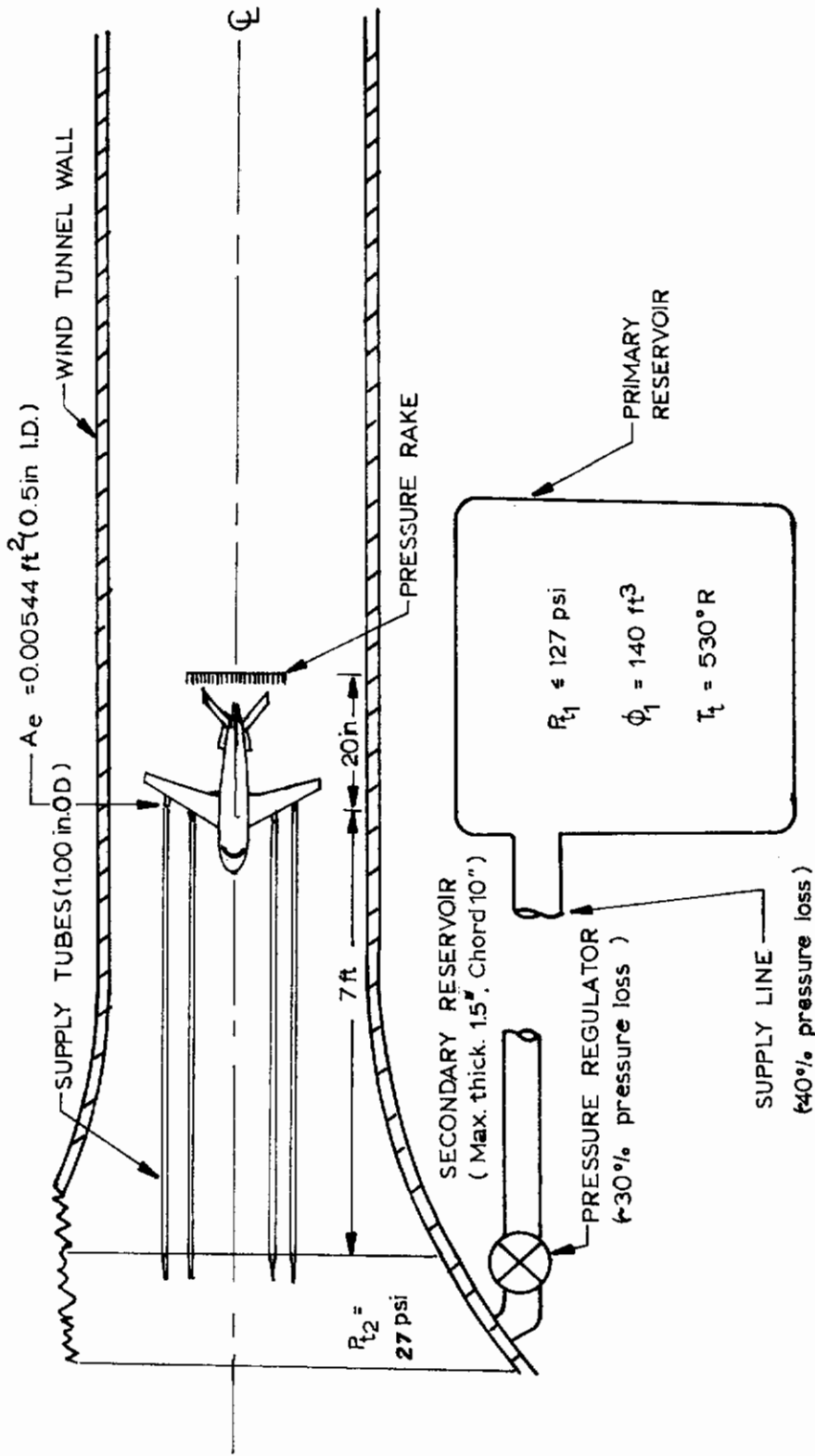
Fig 26 Test Configuration of Power Simulation Apparatus

37

Table I

Values of Pressure Coefficients for Surface Pressure Studies

a) Closed - door Configuration

TAP NO.	C_P	TAP NO.	C_P
1	-0.05	13	-0.06
2	-0.05	14	-0.15
3	-0.05	15	-0.04
4	-0.10	16	-0.03
5	-0.04	17	-0.07
6	-0.06	18	-0.14
7	-0.08	19	-0.02
8	-0.11	20	-0.00
9	-0.05	21	-0.03
10	-0.15	22	-0.01
11	-0.09	23	-0.04
12	-0.09	24	-0.00

b) Open door Configuration

TAP NO.	C_P	TAP NO.	C_P
1	0.00	13	-0.15
2*	0.00	14***	-0.24
3	+0.07	15	-0.14
4	-0.04	16	-0.02
5	+0.12	17	-0.21
6**	-0.39	18***	-0.18
7**	-0.39	19	-0.16
8	+0.06	20	-0.15
9***	-0.66	21***	-0.19
10	-0.10	22	-0.12
11	+0.02	23	-0.24
12	-0.23	24	-0.18

*Opposite Tap #1
**Inside, Near Ramp
***Inner Surface of Doors

Table II

Wake Survey Data at Station 2000

Z = -168		Z = -84		Z = 0				Z = 84				Z = 168			
Y	q/q_∞	Y	q/q_∞	Y	q/q_∞	Y	q/q_∞	Y	q/q_∞	Y	q/q_∞	Y	q/q_∞	Y	q/q_∞
-315.7	1.00	-295.7	1.00	-294.0	1.00	-295.6	0.99	-304.1	1.01	-287.3	1.00	-300.7	1.00	-285.6	1.00
-233.4	1.00	-213.4	0.98	-211.7	0.92	-211.7	0.92	-221.8	1.01	-205.0	1.00	-218.4	1.00	-218.4	1.00
-192.2	0.99	-171.4	1.00	-169.7	0.96	-169.7	0.95	-179.8	1.00	-163.0	1.00	-178.0	1.00	-161.3	0.99
-164.6	0.98	-144.5	0.99	-142.8	0.96	-144.5	0.97	-152.9	0.99	-136.1	0.91	-151.2	0.99	-134.4	0.99
-137.3	0.97	-117.6	0.93	-115.9	0.52	-115.9	0.57	-126.0	0.89	-109.2	0.76	-122.6	0.96	-107.5	0.99
-109.9	0.98	-89.0	0.78	-87.4	0.26	-89.0	0.23	-97.4	0.79	-80.6	0.66	-95.8	0.98	-79.0	0.97
-82.3	0.96	-62.2	0.77	-60.5	0.24	-62.2	0.22	-70.6	0.70	-53.8	0.56	-67.2	0.97	-52.1	0.90
-54.9	1.00	-35.3	0.96	-33.6	0.63	-33.6	0.62	-43.7	0.54	-26.9	0.45	-40.3	0.93	-25.2	0.84
-43.8	0.96	-23.5	0.99	-21.8	0.84	-23.5	0.82	-31.9	0.51	-15.1	0.43	-30.2	0.92	-13.4	0.79
-32.9	0.96	-13.4	1.00	-11.8	0.92	-11.8	0.88	-21.8	0.46	-5.04	0.38	-18.5	0.87	- 3.4	0.59
-22.0	0.99	- 1.7	0.94	0.0	0.86	1.7	0.81	-10.1	0.37	6.72	0.33	- 8.4	0.69	8.4	0.68
-10.9	0.96	8.4	0.97	10.1	0.88	11.1	0.85	0.8	0.35	18.5	0.34	- 3.4	0.65	20.2	0.85
-0.0	0.99	20.2	0.97	21.8	0.74	20.2	0.75	11.8	0.35	28.6	0.40	13.4	0.86	30.2	0.91
10.9	0.99	30.2	0.95	31.9	0.59	31.9	0.62	23.5	0.41	38.6	0.49	25.2	0.92	40.3	0.94
22.0	0.99	42.0	0.93	43.7	0.45	43.7	0.48	33.6	0.51	50.4	0.60	37.0	0.95	52.1	0.97
32.9	0.99	53.8	0.69	55.4	0.37	53.8	0.38	45.4	0.71	62.2	0.70	47.0	0.97	63.8	0.98
43.8	0.99	63.8	0.59	65.5	0.34	63.8	0.32	51.7	0.72	72.2	0.77	58.8	0.97	73.9	0.98
54.9	0.98	75.6	0.53	77.2	0.35	75.6	0.32	67.2	0.90	84.0	0.83	68.9	0.96	85.7	0.97
82.3	1.00	102.5	0.74	104.2	0.61	102.5	0.60	94.1	0.93	112.6	0.94	97.4	0.98	112.6	0.99
109.9	1.00	129.4	0.94	131.0	0.92	131.0	0.93	121.0	0.97	137.8	0.98	124.3	0.98	139.4	0.98
137.3	1.00	157.9	0.98	159.6	0.98	157.9	0.96	149.5	0.99	166.3	1.00	154.6	0.99	168.0	0.99
164.6	1.01	184.8	0.99	186.5	0.91	184.8	0.91	176.4	0.99	193.2	1.00	178.1	1.00	194.9	1.00
192.2	1.01	211.7	1.00	213.4	0.93	213.4	0.93	203.3	1.00	220.1	1.01	206.6	1.00	221.8	1.00
233.4	1.01	253.7	0.87	255.4	0.89	253.7	0.88	245.3	1.00	262.1	1.00	247.0	1.00	263.8	0.99
315.7	1.00	336.0	1.00	337.7	0.99	336.0	1.00	327.6	1.00	344.4	1.00	329.3	1.00	346.1	1.00
Run No. (120)		(135)		(136)		(143)		(144)		(151)		(152)		(159)	

39

Table II

Wake Survey Data at Station 2175

Z = -84

Y	q/q∞
-289.0	1.00
-205.6	0.94
-164.6	1.00
-137.8	0.96
-110.9	0.89
-82.3	0.83
-55.4	0.82
-28.6	0.96
-16.8	1.00
-6.7	1.00
5.0	0.96
16.8	0.99
26.9	0.96
37.0	0.91
48.7	0.81
60.5	0.66
70.6	0.60
82.3	0.56
109.2	0.70
136.1	0.89
164.6	0.97
191.5	0.98
218.4	0.98
260.4	0.84
342.7	0.99
(129)	(134)

Z = 0

Y	q/q∞	Y	q/q∞
-277.2	1.00	-280.6	1.00
-194.9	0.93	-198.2	0.93
-154.6	0.98	-156.2	0.99
-127.7	0.90	-129.4	0.87
-99.1	0.51	-102.5	0.48
-72.2	0.30	-73.9	0.30
-43.7	0.29	-47.0	0.32
-16.8	0.67	-20.2	0.74
-6.7	0.87	-8.4	0.91
5.0	0.96	1.7	0.97
15.1	0.90	13.4	0.89
26.9	0.90	25.2	0.83
37.0	0.69	35.3	0.62
48.7	0.52	45.4	0.47
60.5	0.41	57.1	0.39
70.6	0.37	68.9	0.38
82.3	0.38	79.0	0.39
92.4	0.41	90.7	0.53
121.0	0.63	117.6	0.66
147.8	0.91	144.5	0.92
157.9	0.98	173.0	0.98
201.6	0.92	200.0	0.93
230.2	0.94	226.8	0.95
270.5	0.89	268.8	0.89
352.8	0.99	351.1	0.99
(137)		(142)	

Z = 84

Y	q/q∞	Y	q/q∞
-277.2	1.00	-268.8	1.00
-194.9	1.00	-186.5	1.00
-154.6	0.99	-144.5	0.91
-127.7	0.92	-117.6	0.85
-99.1	0.78	-90.7	0.71
-72.2	0.69	-62.2	0.62
-47.0	0.60	-35.3	0.58
-16.8	0.53	-8.4	0.53
-6.7	0.51	3.4	0.51
5.0	0.48	13.4	0.47
15.1	0.42	25.2	0.41
26.9	0.42	37.0	0.41
37.0	0.42	47.0	0.44
48.7	0.48	57.1	0.50
60.5	0.56	68.9	0.69
70.6	0.65	80.6	0.68
82.3	0.73	90.7	0.75
92.4	0.80	102.5	0.81
121.0	0.92	129.4	0.92
147.8	0.97	156.2	0.97
174.7	0.99	184.8	0.99
201.6	1.00	211.7	0.99
230.2	1.00	238.6	1.00
270.5	0.99	280.6	0.99
352.8	1.00	362.9	1.00
(145)		(150)	

Z = 168

Y	q/q∞	Y	q/q∞
-275.5	1.00	-282.2	1.00
-193.2	1.00	-200.0	1.00
-152.9	0.99	-157.9	0.99
-124.3	0.99	-131.0	0.98
-97.4	0.96	-104.2	0.96
-70.6	0.95	-75.6	0.94
-43.7	0.89	-48.7	0.88
-15.1	0.78	-21.8	0.86
5.0	0.69	-10.1	0.78
6.7	0.70	6.7	0.66
16.8	0.80	11.8	0.76
28.6	0.90	23.5	0.88
40.3	0.94	33.6	0.90
50.4	0.97	43.7	0.93
62.2	0.98	55.4	0.96
72.2	0.98	57.2	0.97
84.0	0.98	77.3	0.98
94.1	0.97	89.0	0.97
121.0	0.99	115.9	0.99
149.5	0.99	142.8	0.99
176.4	1.00	171.4	1.00
205.0	1.00	198.2	1.00
231.8	1.00	225.1	1.00
272.2	1.00	267.1	1.00
354.5	1.00	349.4	1.00
(153)		(158)	

Run No.

40

Table IV

Wake Survey Data at Station 2470

Z = -84

Y	q/q∞	Y	q/q∞
-267.1	1.01	-260.4	1.00
-184.8	0.94	-178.1	0.94
-142.8	0.95	-136.1	0.98
-115.9	0.89	-109.2	0.94
-90.7	0.82	-82.3	0.88
-60.5	0.84	-53.8	0.91
-33.6	0.97	-26.9	1.00
6.7	0.99	0.0	1.00
5.0	1.00	11.8	1.02
15.1	0.94	21.8	1.02
26.9	0.92	33.6	0.94
37.0	0.80	45.4	0.95
48.7	0.72	55.4	0.89
60.5	0.65	67.2	0.82
70.6	0.64	77.3	0.76
82.3	0.66	89.0	0.73
92.4	0.49	99.1	0.71
104.2	0.81	110.9	0.82
131.0	0.91	137.8	0.91
157.9	0.91	164.6	0.91
186.5	0.98	193.2	0.97
213.4	0.99	220.1	0.99
240.2	0.92	247.0	0.94
282.2	0.91	289.0	0.88
364.6	0.99	371.3	0.99

Run No. (130)   (133)

Z = 0

Y	q/q∞	Y	q/q∞
-268.8	1.06	-268.8	1.03
-186.5	1.02	-186.5	1.00
-144.5	0.92	-144.5	0.92
-117.6	0.73	-117.6	0.73
-92.4	0.57	-92.4	0.56
-62.2	0.49	-62.2	0.49
-35.3	0.67	-35.3	0.66
8.4	0.95	8.4	0.94
3.4	0.97	3.4	0.96
13.4	0.89	13.4	0.88
25.2	0.70	25.2	0.70
37.0	0.60	37.0	0.61
47.0	0.51	47.0	0.51
57.1	0.48	57.1	0.48
68.9	0.50	68.9	0.49
80.6	0.54	80.6	0.53
90.7	0.61	90.7	0.59
102.5	0.64	102.5	0.63
129.4	0.81	129.4	0.80
156.2	0.95	156.2	0.94
184.8	1.00	184.8	0.99
211.7	1.01	211.7	0.99
238.6	0.96	238.6	0.94
280.6	0.92	280.6	0.90
362.9	0.94	362.9	0.96

(138)   (141)

Z = 84

Y	q/q∞
-262.1	1.00
-179.8	1.00
-137.8	0.90
-110.9	0.76
-84.0	0.67
-55.4	0.62
-28.6	0.71
1.7	0.76
10.1	0.75
20.2	0.71
31.9	0.61
42.0	0.59
53.8	0.56
65.5	0.56
75.6	0.60
87.4	0.67
97.4	0.73
109.2	0.82
136.1	0.91
163.0	0.96
191.5	0.99
218.4	0.99
245.3	1.00
287.3	0.99
369.6	0.99

(149)

Z = 168

Y	q/q∞	Y	q/q∞
-277.2	1.00	-277.2	1.00
-194.9	1.00	-194.9	1.00
-152.9	0.99	-152.9	0.99
-126.0	0.99	-126.0	0.99
-99.1	0.97	-99.1	0.97
-70.6	0.96	-70.6	0.94
-43.7	0.91	-43.7	0.87
-16.8	0.83	-16.9	0.79
-5.0	0.80	-5.0	0.77
5.0	0.76	5.0	0.74
16.8	0.73	16.8	0.72
28.6	0.82	28.6	0.82
38.6	0.90	38.6	0.89
48.7	0.93	48.7	0.93
60.5	0.96	60.5	0.96
72.2	0.97	72.2	0.97
82.3	0.98	82.3	0.97
94.1	0.96	94.1	0.96
121.0	0.98	121.0	0.98
147.8	0.99	147.8	0.98
176.4	1.00	176.4	0.99
203.3	1.00	203.3	1.00
230.2	1.00	230.2	1.00
272.2	1.00	272.2	0.99
354.5	1.00	354.5	1.00

(154)   (159)

41

Table V

Wake Survey Data at Station 2750

Z = -84

Y	q/q∞ (131)	q/q∞ (132)
-257.0	0.99	1.00
-147.7	0.93	0.92
-132.7	0.93	0.93
-105.8	0.91	0.90
-79.0	0.87	0.87
-50.4	0.91	0.92
-23.5	1.00	1.00
3.4	1.03	1.02
15.1	1.00	1.02
25.2	0.99	0.99
37.0	0.89	0.89
47.0	0.88	0.89
58.8	0.81	0.82
68.9	0.78	0.79
80.6	0.76	0.76
92.4	0.76	0.78
102.5	0.77	0.78
114.2	0.78	0.78
141.1	0.86	0.86
168.0	0.90	0.89
196.6	0.93	0.93
223.4	0.92	0.92
250.3	0.89	0.89
292.3	0.97	0.96
374.6	1.00	1.00

Z = 0

Y	q/q∞ (139)	q/q∞ (140)
-255.4	1.08	1.08
-173.0	1.04	1.04
-131.0	0.87	0.87
-104.2	0.75	0.75
-77.3	0.64	0.65
-48.7	0.66	0.67
-21.8	0.87	0.86
5.0	0.91	0.91
16.8	0.87	0.87
26.9	0.78	0.97
38.6	0.65	0.66
50.4	0.63	0.64
60.5	0.61	0.61
70.6	0.62	0.62
82.3	0.64	0.64
94.1	0.68	0.68
104.2	0.73	0.78
115.9	0.76	0.76
142.8	0.89	0.89
169.7	0.98	0.98
198.2	1.05	1.05
225.1	1.05	1.06
252.0	1.00	0.99
294.0	1.02	1.01
376.3	0.92	0.92

Z = 84

Y	q/q∞ (147)	q/q∞ (148)
-243.6	1.02	1.02
-161.3	0.98	0.98
-119.3	0.83	0.83
-92.4	0.71	0.71
-65.5	0.63	0.62
-37.0	0.65	0.65
-10.1	0.74	0.75
16.8	0.72	0.72
28.6	0.72	0.72
38.6	0.68	0.68
50.4	0.62	0.62
60.5	0.63	0.63
72.2	0.65	0.64
82.3	0.68	0.67
94.1	0.73	0.72
105.8	0.79	0.78
115.9	0.84	0.84
127.7	0.88	0.88
154.6	0.97	0.92
181.4	1.00	0.99
210.0	1.01	1.01
236.9	1.02	1.01
263.8	1.02	1.01
305.8	1.01	1.01
388.1	0.98	0.98

Z = 168

Y	q/q∞ (155)	q/q∞ (156)
-282.4	1.00	1.00
-199.9	1.00	1.00
-157.9	0.98	0.98
-131.0	0.95	0.95
-104.2	0.99	0.88
-75.6	0.82	0.82
-48.7	0.78	0.78
-21.8	0.73	0.72
-10.1	0.74	0.74
0.0	0.74	0.72
11.8	0.73	0.72
23.5	0.79	0.79
33.6	0.85	0.84
43.7	0.89	0.89
55.4	0.93	0.91
67.2	0.96	0.95
77.3	0.97	0.97
89.0	0.96	0.95
115.9	0.99	0.99
142.8	0.99	0.99
171.4	1.00	1.00
198.2	1.00	1.00
225.1	1.00	1.00
267.1	1.00	0.99
349.4	1.00	1.00

Run No. (131)

42

DOCUMENT CONTROL DATA - R & D

(Security classification of title, body of abstract and indexing annotation must be entered when the overall report is classified)

1. ORIGINATING ACTIVITY *(Corporate author)*	2a. REPORT SECURITY CLASSIFICATION
University of Minnesota Minneapolis, Minn. 55455	Unclassified
	2b. GROUP N/A

3. REPORT TITLE

Wind Tunnel Studies of the Pressure Distribution and the Flow Field in the Wake of the Lockheed C-141A Starlifter Jet Transport Aircraft

4. DESCRIPTIVE NOTES *(Type of report and inclusive dates)*
Final Report August 1966 - June 1967

5. AUTHOR(S) *(First name, middle initial, last name)*

T. F. Goodrick

6. REPORT DATE	7a. TOTAL NO. OF PAGES	7b. NO. OF REFS
May 1968	42	3

8a. CONTRACT OR GRANT NO. F33615-67-C-1010	9a. ORIGINATOR'S REPORT NUMBER(S)
b. PROJECT NO. 6065	
c. Task No. 606503	9b. OTHER REPORT NO(S) *(Any other numbers that may be assigned this report)*
d.	AFFDL-TR-67-163

10. DISTRIBUTION STATEMENT This document is subject to special export controls and each transmittal to foreign governments or foreign nationals may be made only with prior approval of the Vehicle Equipment Division (FDF), AF Flight Dynamics Laboratory, Wright-Patterson AFB, Ohio.

11. SUPPLEMENTARY NOTES	12. SPONSORING MILITARY ACTIVITY
	AFFDL (FDFR) Wright-Patterson AFB, Ohio

13. ABSTRACT

Wind tunnel studies of a 1:56 scale non-powered model of the Lockheed C-141A Starlifter jet transport indicate the following characteristics of the flow field which affect the deployment of paratroops and cargo from the side doors and from the rear cargo ramp: a 15° to 20° downwash occurs across the side doors when the petal doors are closed, the flow beneath the side doors is inclined toward the centerline approximately 30°; and a 20° to 40° upwash occurs between and behind the petal doors when the doors are open 65°. An analytic approximation of the effect of engine exhaust on the wake shows that the performance of a single parachute may not be significantly affected, but that of clustered extraction parachutes would be influenced by the engine slipstream.

The distribution of this Abstract is unlimited.

DD FORM 1 NOV 65 1473

14. KEY WORDS	LINK A		LINK B		LINK C	
	ROLE	WT	ROLE	WT	ROLE	WT
Wind Tunnel Tests						
C-141A Aircraft						
Flow Field Studies						
Troop Deployment						
Cargo Extraction						
Aircraft Wake						